HELSINKI UNIVERSITY OF TECHNOLOGY
Department of Electrical and Communications Engineering
Communications Laboratory

Decision Feedback Equalization in OFDM with Long Delay Spreads

Zeeshan Ahmed Qureshi

Masters Thesis submitted in partial fulfilment of the requirements for the Degree of Masters of Science in Technology

Espoo, 30th of May 2008

Supervisor: Professor Olav Tirkkonen

Instructor: Professor Olav Tirkkonen

HELSINKI UNIVERSITY OF TECHNOLOGY **Abstract of the Master's Thesis**

Author: Zeeshan Ahmed Qureshi

Title: Decision Feedback Equalization in OFDM with Long Delay Spreads

Date: May 30, 2008 **Number of pages:** 68 + 22

Faculty: Electronics, Communications and Automation

Professorship: S-72 Communications Engineering

Supervisor: Professor Olav Tirkkonen

Instructor: Professor Olav Tirkkonen

Abstract

OFDM-based Single Frequency Networks (SFN) used in DVB-T broadcasting offer many advantages and have become the standard solution being adopted in Europe. However, at the receiver, the simultaneous data transmission from the multiple transmitters in an SFN is interpreted as a channel with a long delay spread. The multiple signals being received at delayed intervals cause an increase in interference components that cause errors in symbol recovery.

In order to recover from performance degradation inherent in such channels with long delay spreads, this thesis discusses a receiver design based on the implementation of a Decision Feed-back Equalizer (DFE). The proposed DFE receiver incorporates a Parallel Interference Canceller (PIC) as its feed-forward filter. This simple combination enables better symbol recovery while maintaining a simple receiver design.

In this thesis the simulation performance of the proposed DFE receiver is investigated in comparison to the conventional OFDM receiver. In order to implement SFN scenarios, multipath Rayleigh fading channels with long delay spreads are selected as the wireless communication medium. The evaluation is done in a simulator developed in MATLAB.

Keywords: OFDM, Single Frequency Network (SFN), DVB-T, Decision Feedback Equalization (DFE), Parallel Interference Cancellation (PIC)

TEKNILLINEN KORKEAKOULU **Diplomityön tiivistelmä**

Tekijä: Zeeshan Ahmed Qureshi

Työn nimi: Decision Feedback Equalization in OFDM with Long Delay Spreads

Päiväys: 30. toukokuuta 2008 **Sivumäärä** 68 + 22

Tiedekunta: Elektroniikan, tietoliikenteen ja automaation tiedekunta

Professuuri: S-72 Tietoliikennetekniikka

Työn valvoja: Professori Olav Tirkkonen

Työn ohjaaja: Professori Olav Tirkkonen

Tiivistelmä

OFDM:ään perustuvat yhden taajuuden verkot (SFN), joita käytetään DVB-T yleisradiolähetyksissä tarjoavat monia etuja. Niistä on tullut standardiratkaisu digitaalisten televisiolähetysten tuottamiseen Euroopassa. Vastaanottimessa yhtäaikaiset lähetykset monista SFN:n monista lähettimistä näyttävät kanavalta, jolla on pitkä viivehaje. Viivästettyinä vastaanotettavat signaalit lisäävät interferenssiä vastaanotossa, ja osaltaan lisäävät vastaanotossa tapahtuiva virheitä.

Tässä työssä tarkastellaan mahdollisuutta parantaa vastaanottimen toimintaa pitkän viivehajeen kanavissa käyttäen päätöstakaisinkytkentää (DFE). Ehdotettu DFE-vastaanotin sisältää rinnakkaisen interferenssinpoistajan (PIC) feedforward-suotimenaan. Tämä yhdistelmä parantaa symbolin vastaanottoa ilman että vastaanottimen kompleksisuus lisääntyy kohtuuttomasti.

Työssä tutkitaan ehdotetun DFE-vastaanottimen toimintaa simulaatioin, ja verrataan sen suorituskykyä tavanomaiseen OFDM—vastaanottimeen. SFN-skenaarioita mallinnetaan monitappisilla Rayleigh-häipyvillä kanavilla, joilla on pitkä viivehaje. Vartailut suoritetaan simulaattorissa joka on kehitetty käyttäen MATLAB-kieltä.

Avainsanat: OFDM, yhden taajuuden verkot, DVB-T, päätöstakaisinkytketty ekvalisointi, rinnakkainen interferenssin poisto

Kieli: Englanti

ACKNOWLEDGEMENTS

I would like to take this opportunity to thank all the people who have helped and guided me throughout my thesis work. First of all, I would like to express my deepest gratitude to Professor Olav Tirkkonen who has shown great interest in my work. I really appreciate the intensive help he has provided me and the immense amount of time he has allocated to guide me.

I would also like to thank my friends Aamir Mahmood, Konstantinos Koufos and Mobien Shoaib who have helped me a lot during the course of the thesis. Their constant support means a lot to me. Most importantly, they have been patient with me while I discussed my thesis work pretending it to be normal conversation.

I would specially like to thank my friend Konstantinos' parents who provided me with Greek coffee to stay awake and work endless nights on my thesis. The coffee has helped me complete the thesis in due time.

Furthermore, I would like to thank my friends Ananda, Bilal, Majid, Naveed, Petteri and Sohail for their continuous moral support and their constant reminder that life needs to be a balance between work and leisure. It means a lot that they cared enough to try and distract me from my thesis.

Finally, and most importantly, I am very grateful to my siblings and my parents for their unconditional love and support, and for their constant encouragement and patience while dealing with me. They have been the pillar of my strength through difficult times and their encouragement has enabled me to complete this work.

30th of May 2008, Espoo – Finland

Zeeshan Ahmed Qureshi

TABLE OF CONTENTS

LIST OF FIGURES

LIST OF TABLES

LIST OF ABBREVIATIONS

AWGN	Additive White Gaussian Noise
BER	Bit Error Ratio
CDF	Cumulative Distribution Function
CDMA	Code-Division Multiple Access
CP	Cyclic Prefix
DFE	Decision Feed-back Equlizer
DVB-T	Digital Video Broadcasting - Terrestrial
FFT	Fast Fourier Transform
HDPIC	Hard-Decision Parallel Interference Canceller
ICI	Inter-Carrier Interference
IFFT	Inverse Fast Fourier Transform
ISD	Inter-Site Distance
ISI	Inter-Symbol Interference
LPIC	Linear Parallel Interference Canceller
MAI	Multiple Access Interference
MLSE	Maximum-Likelihood Sequence Estimation
MMSE	Minimum Mean-Square Error
OFDM	Orthogonal Frequency-Division Multiplexing
PDP	Power Delay Profile
PIC	Parallel Interference Canceller
QPSK	Quadrature Phase-Shift Keying
SFN	Single Frequency Network
SIC	Successive Interference Canceller
SINR	Signal-to-Interference-plus-Noise Ratio
SNR	Signal-to-Noise-Ratio

CHAPTER 1

INTRODUCTION

1.1 MOTIVATION

Modern broadcast networks such as Terrestrial Digital Video Broadcasting (DVB-T) make use of wireless networks where multiple transmitters simultaneously transmit the same Orthogonal Frequency Division Multiplexing (OFDM) data. Such wireless networks are termed as Single Frequency Networks (SFN) and are extensively being used throughout Europe. OFDM modulation is the preferred solution in broadband wireless systems due to its simple equalization and its inherent resistance to interference in multi-path channels.

In such networks, the simultaneous transmission of the same data from multiple transmitters causes the receiver to interpret the channel as one with a long delay spread. The existence of a channel delay spread longer than the cyclic prefix (CP) length causes severe performance degradation due to the contribution of inter-symbol interference (ISI) and inter-carrier interference (ICI) into the received OFDM symbol.

Conventional wisdom dictates that in order to overcome this channel impairment, the CP length be increased to at least the length of the channel delay spread. This technique would permit the increased CP to absorb all of the ISI and ICI components allowing the actual data symbol to be extracted without any errors. This method, however, increases the data symbol overhead and degrades the system efficiency.

Another approach to overcome this problem is the use of time-domain equalization. With time domain equalization the channel impulse response is shortened, allowing the same CP length to absorb the interference components. This allows the system to be efficient; however the method is impractical due to its complex receiver design.

In order to improve performance without increasing the length of the CP or making the system too complex, this thesis proposes a receiver with Decision Feed-back Equalizer (DFE) coupled to a Parallel Interference Canceller (PIC). The proposed scheme allows us to improve the performance of the system without compromising the efficiency of OFDM.

1.2 PROBLEM FORMULATION

The objective of this thesis is to simulate and investigate a PIC-based DFE receiver in downlink broadcast communication systems. Simulation of the proposed receiver is done in worst-case scenario channels with long delay spreads. In addition, the receiver is also tested on simulated SFN channels with different inter-site distances (ISD).

The scope of the thesis is to analyze the performance of the proposed receiver against the performance of a conventional OFDM receiver. The receiver performance is investigated over various channel delay spreads. The response of the proposed receiver to its various parameters is also observed and analyzed. To this end, various configurations of the proposed receiver are implemented and their effect on symbol recovery is analyzed.

The performance of the receivers is measured in terms of their bit error ratio (BER) through variation of the signal-to-noise ratio (SNR). The receivers are compared along various scenarios and their performance is critically evaluated.

The aim of the thesis is to advance our understanding of communication in channels with long delay spreads and to justify the implementation of the proposed receiver as a means to recover from its performance degrading effects.

1.3 STRUCTURE OF THE THESIS

The thesis has been structured into the following chapters that are shortly outlined below:

Chapter 2: This chapter deals with the theoretical review of the basic technologies involved within the thesis work. It describes the basics of channel models, OFDM and SFN.

Chapter 3: This chapter introduces the various receiver equalization techniques being utilized in this thesis work. It covers the topics of DFE equalizer and the PIC detector in detail due to their essential role in this thesis.

Chapter 4: This chapter provides a brief overview of the related work that has been done along the line of our topic. It illustrates some of the important technical papers related to research done in this field.

Chapter 5: This chapter deals with the details of the simulation work done as part of this thesis. It discusses the simulator model, the receiver design, the simulation parameters and its implementation.

Chapter 6: This chapter details the performance results achieved from the receiver implementation. It furthermore discusses and analyzes the behaviour of the results.

Chapter 7: This chapter draws conclusions from the work done and provides an overall analysis.

1.4 BASIC DEFINITIONS

- **Inter-Site Distance (ISD)**

  The inter-site distance (ISD) defines the distance between two neighbouring BSs and it is a fixed value. Changing the ISD affects the way signals interact at the receiver.

- **Cellular Network Structure**

  The network structure is based on hexagonal cells. Each of the cells has a transmitted in its centre catering to the users in that cell. A cellular network structure is shown in Figure 1.1 [1]. In this thesis, transmitters from surrounding cells also cater to the receiver in a particular cell.

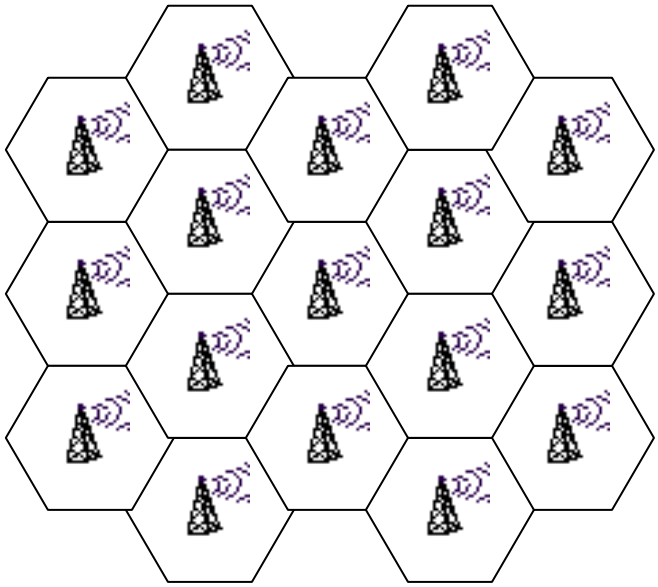

Figure 1.1: Cellular Structure of the Network

- **Broadcasting**

  Broadcasting refers to transmission of communication signals to users located inside the broadcast coverage area. The signals are accessible by all devices located in such an area. Television and radio communication is based on broadcasting signals.

- **Modulation**

  Modulation is the mapping of information to changes in the carrier signal's phase, frequency or amplitude. The aim of modulation is to transfer data over a medium in such a way that it is easily recognisable and retrievable at the receiving end [2].

- **Multiplexing**

  Multiplexing is the method of sharing bandwidth with other independent data channels. The aim of multiplexing is to share a limited resource between multiple contenders of that resource [2].

- **Bit Error Ratio (BER)**

  Bit Error Ratio is the ratio of the number of bits incorrectly received at the receiver to the total number of bits transmitted during a certain time interval.

- **Signal-to-Noise-Ratio (SNR)**

  SNR is a ratio between the signal power to the noise power reaching the receiver. It is a performance measure for the quality of service the network provides to a user.

- **DVB-T**

  Digital Video Broadcasting – Terrestrial (DVB-T) is the European consortium standard for the broadcast transmission of digital terrestrial television. This system transmits a compressed digital audio/video stream using OFDM modulation with concatenated channel coding (COFDM) [3].

CHAPTER 2

THEORETICAL REVIEW

2.1 CHANNEL MODEL

In order to evaluate the performance of a communication system, an accurate description of the wireless channel is required to address its propagation environment. The radio architecture of a communication system plays a very significant role in the modeling of a channel [4]. This thesis work relates to a DVB-T transmission system where the transmitters and receivers remain stationary.

The major role players in such a wireless channel are:

- **Path Loss**

  Path loss is affected by several factors including distance between the transmitter and the receiver, propagation medium, the height and location of antennae, the frequency bandwidth in use, etc.

- **Shadow Fading**

  Shadow fading is fading where the amplitude and phase change remain roughly constant over the period of symbol transmission. It is caused due to the presence of large obstructions lying between the signal path of the transmitter and the receiver. It varies with the environment where the network is being implemented due to terrain contours, vegetation, the presence of buildings, etc.

- **Multi-path Fading**

  Multi-path fading results due to the scattering nature of the environment. Non-line-of-sight (NLOS) propagation in the wireless channel allows the same signal to traverse through different paths and reach the receiver at different timings with varied amplitudes and phases. The receiver sees the channel as a delayed channel where the transmitted symbols keep arriving later than a line of sight symbol would. Delay spread is a parameter used to signify the effect of multi-path propagation and it depends on the terrain, distance, antenna directivity, etc. [4]

- **Doppler Spread**

  The Doppler spread is another factor that affects transmission through a channel. It comes into effect due to the motion of either the receiver or the transmitter relative to each other. However since the receiver and the transmitter are stationary in the context of this thesis, Doppler spread can be assumed as negligible. It should be kept in mind that movement of reflective objects in the environment may also cause this effect and as such, there is always some amount of Doppler spread present.

- **Types of Fading Channels**

  The Rayleigh fading channel consists of small-scale fading due to the presence of numerous reflective paths in the channel. There is an absence of any line-of-sight signal component in this type of channel and the envelope of its received signal is statistically described by a Rayleigh pdf. When a line-of-sight propagation path is present, the small-scale fading is described by a Rician pdf. [4] [8]

  This thesis makes use of a Rayleigh channel. This is because the SFN environment is made up of multiple transmitters transmitting the same data simultaneously from their respective positions. The receiver interprets this as a situation where only one transmitter has transmitted the signal and multiple copies arrive, each through its own path and with its own delay. Due to the lack of a distinctively high amplitude signal, the receiver interprets it as NLOS propagation and hence, a Rayleigh channel is assumed.

2.2 ORTHOGONAL FREQUENCY DIVISION MULTIPLEXING

OFDM is a digital multi-carrier modulation scheme that employs a large number of orthogonal closely-spaced sub-carriers. Each sub-carrier is modulated with a modulation scheme (QPSK or QAM generally) at a low symbol rate. Each of the sub-carrier is then multiplexed together and this forms the OFDM signal. In practice OFDM signals are generated and detected using the Fast Fourier Transform algorithm [5]. The process of signal generation and detection in OFDM is shown in Figure 2.1 [6].

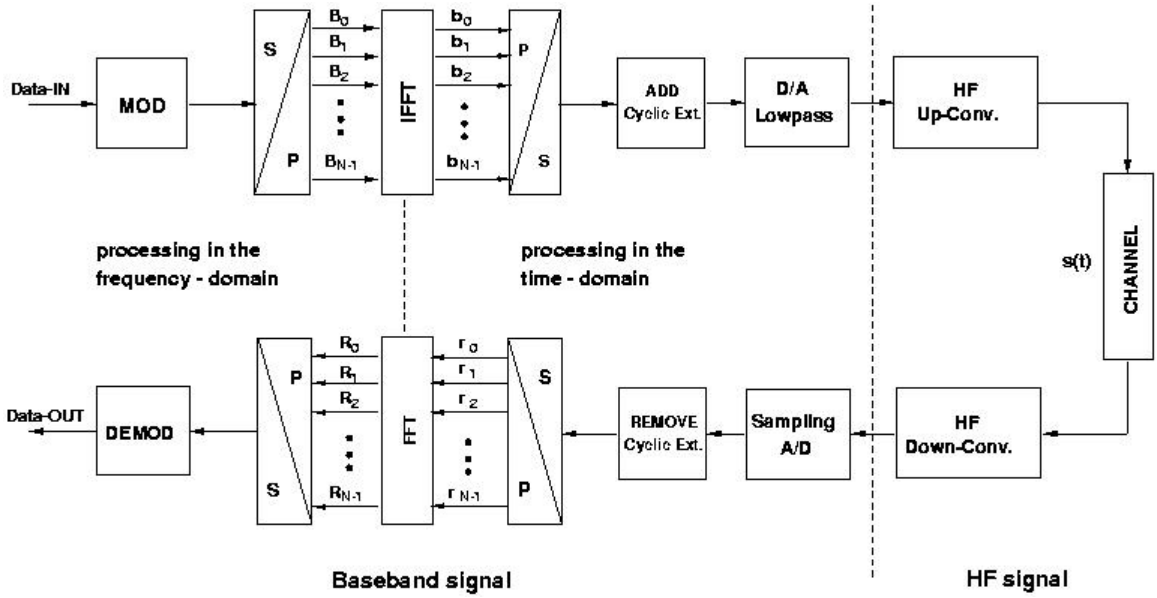

Figure 2.1: Block Diagram of an OFDM based Transmission System

Mathematically, the low-pass equivalent OFDM signal is expressed as in equation 2.1 below:

$$v(t) = \sum_{k=0}^{N-1} X_k e^{\frac{i2\pi kt}{T}}, 0 \le t < T \qquad (2.1)$$

In equation 2.1, X_k are the data symbols, N is the number of sub-carriers and T is the OFDM symbol time [5].

2.2.1 CHARACTERISTICS OF OFDM SIGNALS

The following are the basic characteristics employed in the operation of OFDM:

- **Orthogonality**

  The sub-carrier frequencies are chosen so that they are orthogonal to each other. This means that cross-talk between the sub-carriers is not possible and hence inter-carrier guard bands are not required. This orthogonality allows:

  - simultaneous transmission on numerous sub-carriers in a tight frequency band without interference from each other
  - high spectral efficiency, near the Nyquist rate
  - simpler transmitter and receiver design
  - efficient modulator and demodulator implementation using the FFT algorithm

  However, in order to maintain orthogonality, very accurate frequency synchronization is required between the receiver and the transmitter. If the frequency deviates, the sub-carriers would not remain orthogonal causing inter-carrier interference (ICI) [7]. Figure 2.2 shows three such sub-carriers that are orthogonal to each other [32].

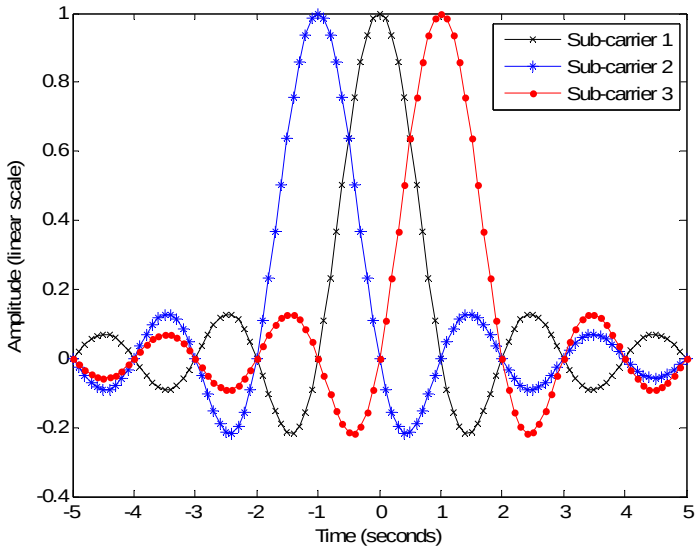

Figure 2.2: Orthogonality of Sub-Carriers

- **Guard Interval**

  OFDM transmits a number of low-rate streams in parallel instead of a single high-rate stream. Lower symbol rate modulation means the symbol duration is comparatively longer and it is feasible to insert a guard interval between OFDM symbols. The presence of this guard interval makes the system resilient to multi-path components and helps eliminate inter-symbol interference (ISI). The guard interval also eliminates the need for a pulse-shaping filter and reduces the sensitivity to time synchronization problems. [5]

- **Cyclic Prefix**

  The cyclic prefix is transmitted during the guard interval and it consists of the end of the OFDM symbol copied into the guard interval. The cyclic prefix is transmitted followed by the OFDM symbol. Cyclic Prefix insertion is shown in Figure 2.3 [5].

  The reason for the cyclic prefix being a copy of the OFDM symbol's tail is so that the receiver will integrate over an integer number of sinusoid cycles for each of the multi-path components when it performs OFDM demodulation with the FFT [5].

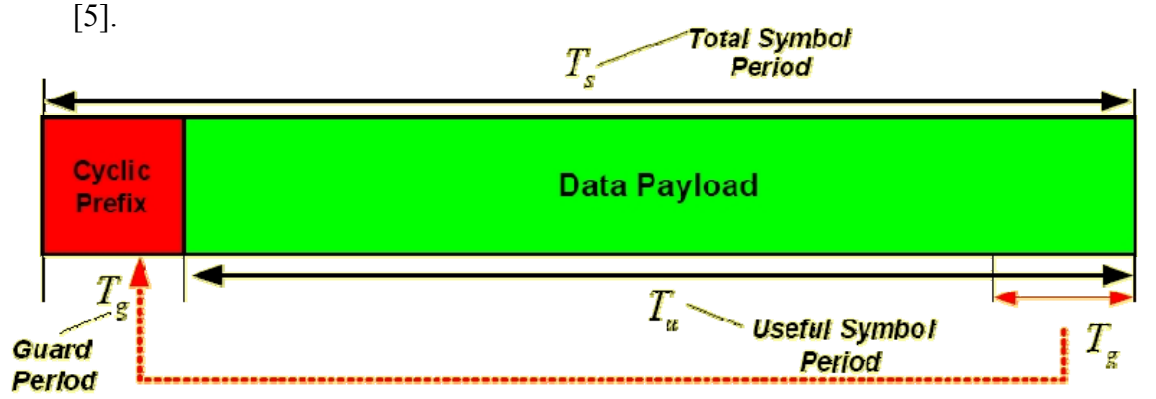

Figure 2.3: Insertion of Cyclic Prefix

- **Simplified Equalization**

  The effects of frequency-selective channel conditions, for example fading caused by multi-path propagation, can be considered as constant (flat) over an OFDM sub-channel if the sub-channel is sufficiently narrow-band, i.e. if the number of sub-channels is sufficiently large. This makes equalization simpler at the receiver in OFDM in comparison to conventional single-carrier modulation. The equalizer

only has to multiply each sub-carrier by a constant value, or a rarely changed value. [5]

- **Pilot Carriers**

  Some of the sub-carriers in OFDM symbols may carry pilot signals for measurement of channel conditions. Pilot signals may also be used for frequency synchronization. [5]

- **Channel Coding and Interleaving**

  OFDM is invariably used in conjunction with channel coding (forward error correction), and almost always uses frequency and/or time interleaving. Frequency interleaving ensures that bit errors resulting from those sub-carriers that are selectively fading are spread out in the bit stream rather than being concentrated. This increases resistance to frequency-selective channel conditions. Similarly time interleaving ensures that bits close together in the bit stream are transmitted further apart in time, thus mitigating against severe fading, as would happen at high speeds. Common types of error correction coding used with OFDM-based systems are convolutional coding, Reed-Solomon coding and turbo coding. Error correction coding is employed in the receiver to correct any errors that result from environmental effects. [5]

2.3 CODED OFDM (COFDM)

Coded OFDM (COFDM) is OFDM that makes use of interleaving and forward error correction (FEC) coding for protection of data against errors. Generally convolutional coding is the type of error correction that is used. Error correction coding provides redundancy to the signal in order for the receiver to be able to correct any bits that are received in error. The error correction decoder in COFDM is the Viterbi algorithm which tries to decode what bits were sent based on the received sampled values.

COFDM also allows different groups of bits to be protected with a different strength code rate. This is done in cases where some bits are more important for the correct reproduction of the signal than other bits, such as the filter parameters in MPEG audio streams. This allows the Viterbi error correction decoder a higher chance of correcting any errors. [9]

2.4 SINGLE FREQUENCY NETWORKS (SFN)

SFN is a broadcast network where several transmitters transmit the same signal simultaneously over the same frequency channel. The aim of SFN is efficient utilization of the radio spectrum, allowing a higher number of radio or television programs to operate in comparison to multi-frequency network (MFN) transmission. It also increases the coverage area and decreases the outage probability in comparison to a MFN since the total received signal strength increases between the transmitters. SFN schemes are somewhat analogous to macro diversity. [10] Figure 2.4 shows a simplified SFN model [11].

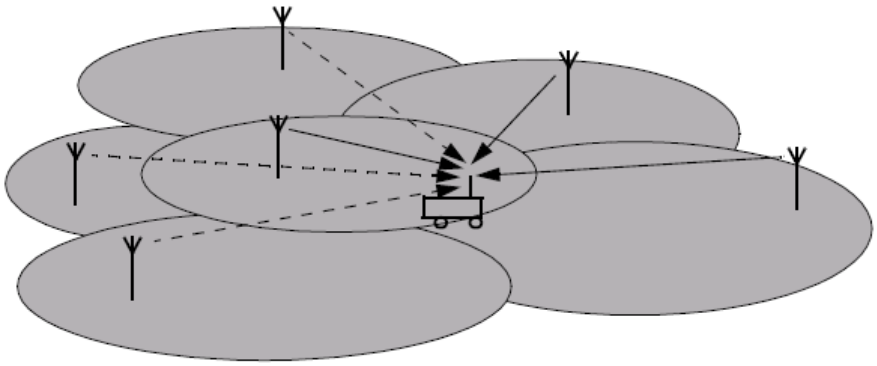

Figure 2.4: Simplified Single Frequency Network Model

In a SFN, the useful signal at the receiver is the superposition of all signals coming from all the transmitters, with different delays. The overall channel is then modeled as a time dispersive channel with a long impulse response that may span a number of symbol periods. This allows the network to obtain a large diversity gain which, in turn, yields a better coverage and frequency economy as compared with analog broadcasting. [11] [12]

2.4.1 TIME DISPERSION PHENOMENON IN SFN

In a SFN, multiple copies of the signals arrive at the receiver antenna with different delays. The time dispersion is caused by two main mechanisms. The "natural dispersion" is caused by wave components reflected by obstacles in the vicinity of the receiver while the "artificial dispersion" derives from the reception of signals from several transmitters placed at different distances from the receiver. The delay of the natural echoes is usually limited to 20-30 micro-seconds corresponding to a difference in the propagation path up to 10 km. Since the symbol duration is very long compared to the natural dispersion, the effects of reflection in the vicinity of the receiver can be neglected. Thus, interference is caused mainly by the artificial delay spread. This is elaborated in figure 2.5 where natural delays are marked with apostrophe signs [11].

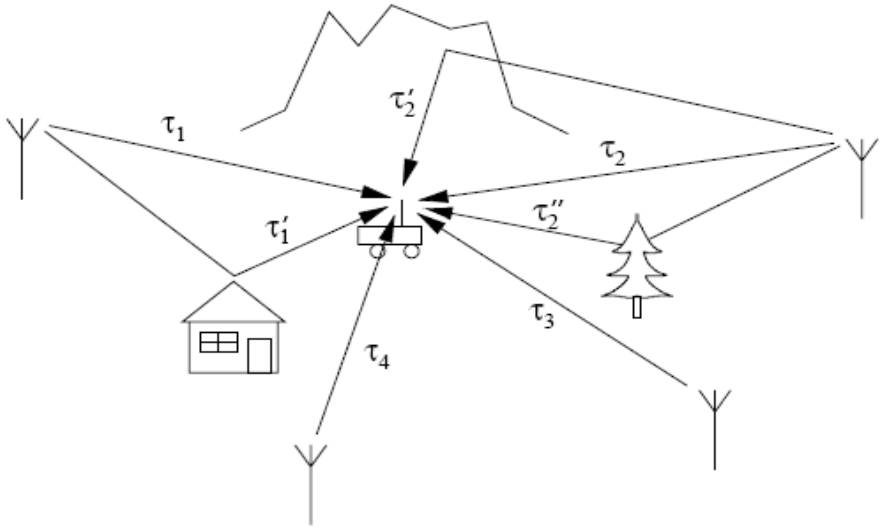

Figure 2.5: Natural and Artificial Delays due to Simulcasting in SFN

In OFDM systems the extreme delay spread is controlled by using a longer transmitted symbol than the actual interval observed by the receiver. If the delay spread of the signal is smaller than the guard interval, no ISI and ICI occurs and the signal contributes totally to the wanted signal. However, symbols of transmitters located far away can cause interference due to the excessive delay. Therefore, in SFNs not only noise but also delayed signals outside the guard interval have an important impact on the achievable coverage. [11]

2.4.2 USE OF 8-VSB MODULATION IN A SFN

SFNs in North America employ 8-level vestigial sideband (VSB) modulation, as specified in the ATSC standard A/110 [10]. The system is relatively good at ghost cancellation but performs poorly in the presence of multi-path. However, advanced technologies are being developed that allows 8-VSB to perform on par to OFDM in a SFN environment. [13]

2.4.3 USE OF COFDM IN SFN

COFDM has been adopted as the standard SFN implementation scheme in DVB-T (used in mainly in Europe), and in ISDB-T (used in Japan and Brazil) [10]. This thesis makes use of simulated channels of COFDM-based SFNs.

In OFDM-based SFN, receivers can benefit from receiving signals from several spatially-dispersed transmitters simultaneously, since transmitters destructively interfere with each other only on a limited number of sub-carriers whereas in general they reinforce coverage over a wide area. This is the implementation of transmitter diversity in OFDM and it allows the available spectrum to be more efficiently utilized compared to MFNs. It also results in a diversity gain. The coverage area is effectively increased while the outage probability decreases in comparison to a MFN [5].

The specifications of DVB-T offer a wide range of operations defined by the number of carriers, the length of the guard interval, modulation scheme and error correcting code with different code rates resulting in different levels of protection. A unique feature of DVB-T standard is the hierarchical transmission where an incoming multiplex is split into two separate streams known as a low priority (LP) and a high priority (HP) stream, both streams with different channel coding and modulation applied. The HP stream provides the basic TV service with relatively low data rate and a high error protection while the LP stream may be used to transmit additional services or to increase the quality of the basic service. [11]

CHAPTER 3

EQUALIZATION TECHNIQUES

3.1 CONVENTIONAL OFDM RECEIVER

In order to gauge the performance of the proposed DFE-PIC equalizer, it is necessary to compare it to the conventional OFDM receiver. The conventional OFDM receiver works on the principle of matched filtering. The matched filter is an optimal linear filter that maximizes the SNR. The matched filter in the receiver is a time-reversed version of the transmitter matched filter. [17]

The matched filter is especially useful with narrow-band transmission where the pulse waveform is spread out in time domain. The filter is able to gather more of the pulse energy that would otherwise get lost in direct sampling. [17]

In conventional OFDM receivers, Fourier transformations and inverse Fourier transformations are used as the matched filters for OFDM. The inverse Fourier transform (IFFT) is implemented over the transmitting signal in the transmitter while the Fourier transform (FFT) is implemented over the received signal in the receiver. This configuration in the transmitter and the receiver forms a matched filter pair and helps recover the OFDM symbol in an optimum manner.

However, if the delay spread of the channel is longer than the CP, interference components breach the transmitted symbol, which the matched filter is unable to combat. In such a scenario, we require additional methods of combating interference. In this thesis, we propose the use of DFE-PIC equalization in the receiver in order to combat interference effects.

3.2 DECISION FEEDBACK EQUALIZER (DFE)

A decision feedback equalizer (DFE) is a non-linear equalizer that uses previous detector decisions to eliminate ISI on the current received symbol [14]. In principle, if a number of source symbols are correctly detected and the channel impulse response is known, then the ISI from these symbols can be reconstructed and cancelled from the current received symbol [15].

The DFE utilizes a feed-forward and a feed-back filter both of which can be linear filters. The non-linearity of the DFE comes with the inclusion of the decision device into the loop. The ISI is cancelled out by the feedback loop while the feed-forward filter mitigates the ICI. The feed-forward filter can be of any type and generally a minimum mean-square error (MMSE) filter is implemented.[16] [14]. In this thesis the feed-forward is implemented in the form of a Parallel Interference Canceller (PIC) detector.

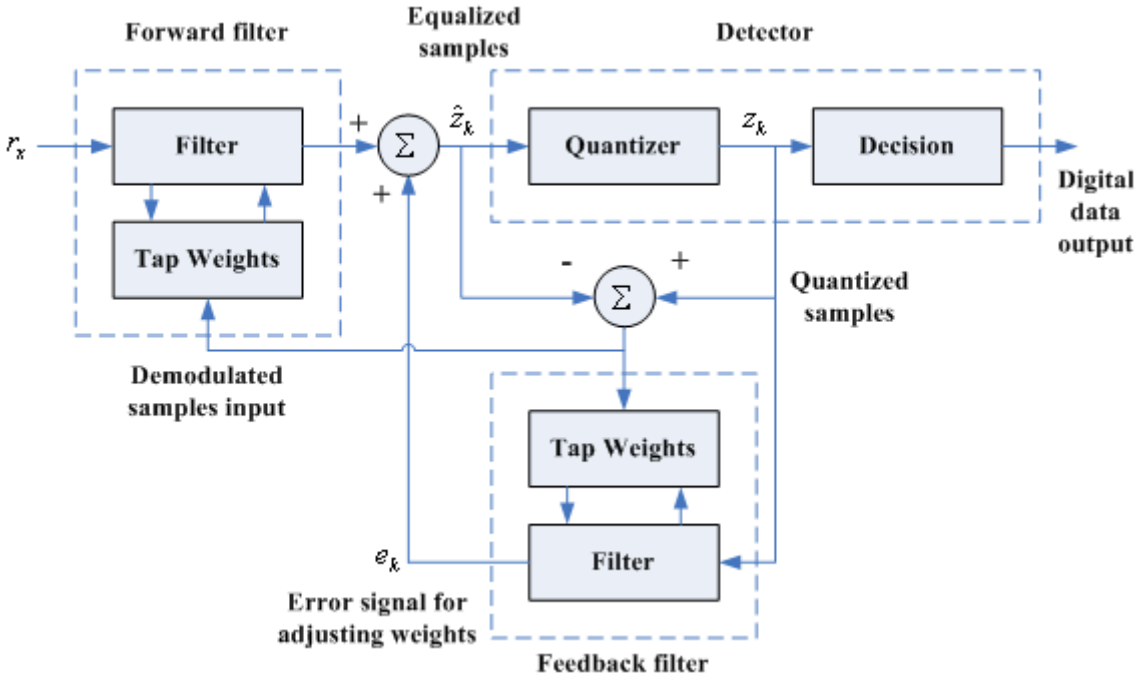

Figure 3.1: Simplified Block Diagram of a DFE

A simplified block diagram of a DFE is shown in figure 3.1 [14]. The figure shows the basic idea of a DFE that the ISI contributed by the previously detected symbols can be cancelled out exactly from the output of the forward filter by subtracting past symbol values with appropriate weighting. The forward and feed-back tap weights can be simultaneously adjusted to fulfill a criterion such as minimizing the mean-square error. [14]

The DFE has a clear advantage over linear equalizers since it has lower noise enhancement while it processes the received signal. The feed-back loop utilizes the detector decisions which are subtracted from the current received symbol and therefore the feed-back signal does not contain any noise components.

3.2.1 ERROR PROPAGATION IN DFE

Error propagation is a major cause of concern in DFE. The design of a DFE is based on the assumption that the detector decisions are correct. However, due to the presence of noise the decisions made cannot always be correct. The presence of a feed-back loop makes the condition serious as an error in the current decision can cause a burst of errors in future symbol decisions.

However, if there are M consecutive correct decisions, where M is the order of the feedback filter, the feed-back part will give appropriate contributions again, and from here on the DFE will operate correctly until the next error. Assuming a binary PAM signal, it can be shown that this happens after K symbols, on average, where

$$K = 2(2^M - 1) \tag{3.1}$$

This gives the average error probability as

$$P_e = 2^M P_{e,0} \tag{3.2}$$

In equation 3.2, $Pe_{,0}$ is the error probability with no error propagation.

It is seen that the DFE error probability grows exponentially with the DFE filter length M. Hence, the feed-back filter length should be kept small in order to guarantee good performance. The error propagation can be kept in control by designing the DFE model with sufficient performance margin to account for the degradation due to error propagation. [17]

In order to resolve the error propagation phenomenon, in practice a typical operation of adaptive DFE detection involves mode switching between a decision-directed blind transmission phase and a training phase. The training sequence phase helps to synchronize the detector decisions avoiding unreliable adaptation. [18]

3.3 MULTI-USER DETECTION

A conventional multi-user system, such as DS-CDMA, MC-CDMA or OFDMA, treats each user separately as the desired signal, with other users considered as noise or multiple-access interference (MAI). The capacity of a system is interference-limited. Specifically in CDMA-based systems, the near/far affect causes performance degradation to those users that are further away from the base station [19]. In an OFDMA system an offset in the carrier frequency synchronization of different users can cause interference between the users. In a single-user OFDM, carrier frequency offset introduces ICI. [20]

Multi-user detection considers all users as signals for each other and implements a method of joint detection of the required signal from the collective received signals [19]. Based on the decisions made from the undesired user signals, MAI is estimated and subtracted from the received signal. This results in the removal of interference of all the other users except for the desired user signal.

In this thesis work, we deal with multiple television channels as opposed to the conventional multiple users in multi-user detection. As such, we eliminate multi-channel interference, or simply ICI instead of MAI, from the received signal. The principle of operation remains the same.

Various techniques have been developed to implement multi-user detection. The major sub-divisions are discussed below, along with a brief explanation:

3.3.1 OPTIMAL MLSE DETECTOR

The objective of the maximum-likelihood sequence estimation (MLSE) is to find the input sequence that maximizes the conditional probability, or likelihood, of the given output sequence [21], [22]. The optimal MLSE detector yields the most likely transmitted sequence by selecting the sequence that maximizes the probability of being transmitted over the complete received message.

Although it provides huge performance and capacity gains over conventional detection, the optimal MLSE detector is not practical. The problem with the approach is the existence of 2^{NK} possible vectors, where N is the typical message length and K

is the number of users. An exhaustive search is clearly impractical for typical message sizes and number of users. The detector can also be implemented with a Viterbi algorithm (for DS-CDMA). Unfortunately the required Viterbi algorithm has a complexity that is still exponential in the number of users, on the order of 2^K. [23]

3.3.2 LINEAR SUBOPTIMAL DETECTORS

This group of multi-user detectors applies a linear mapping to the soft output of the conventional detector to reduce the MAI seen by each user [23]. The most important linear suboptimal detectors are discussed below briefly:

3.3.2.1 Decorrelating Detector

The decorrelating detector applies the inverse of the correlation matrix to the conventional detector output in order to decouple the data. This detector has the capacity to completely eliminate MAI and has less computational complexity than the optimal MLSE detector. However, it causes noise enhancement to the processed signal and the computations needed to invert the correlation matrix are difficult to perform in real time. [23] Additional explanation can be found in [24], [22], [25].

3.3.2.2 Minimum Mean-Squared Error (MMSE) Detector

The MMSE detector takes into account the background noise and utilizes knowledge of the received signal powers. It implements linear mapping which minimizes the mean-squared error between the actual data and the soft output of the conventional detector.

The MMSE detector makes use of a partial or modified inverse of the correlation matrix, The amount of modification is directly proportional to the background noise; the higher the noise level, the less complete an inversion can be done without noise enhancement causing performance degradation. Thus, the MMSE detector balances the desire to decouple the users and completely eliminate MAI with the desire to not enhance the background noise.

Because it takes the background noise into account, the MMSE detector generally provides better probability of error performance than the decorrelating detector. Like the decorrelating detector, the MMSE detector faces the task of implementing the

correlation matrix inversion computation of which is difficult to implement in real time. However, unlike the decorrelating detector, it requires estimation of the received amplitudes and, its performance depends on the powers of the interfering users [23]. Additional explanation can be found in [26].

3.3.3 NON-LINEAR SUBOPTIMAL DETECTORS

This group of multi-user detectors utilizes interference cancellation methods which apply feedback to reduce MAI in the received signal [22]. The basic principle underlying these detectors is the creation at the receiver of separate estimates of the MAI contributed by each user in order to subtract out some or all of the MAI seen by each user. Such detectors are often implemented with multiple stages, where the expectation is that the decisions will improve at the output of successive stages.

The bit decisions used to estimate the MAI can be hard or soft. The soft-decision approach uses soft data estimates for the joint estimation of the data and amplitudes. It is relatively easier to implement and is also referred to as a linear SIC/PIC since soft-decisions are utilized. The hard-decision approach feeds back a hard bit decision and are referred to as non-linear SIC/PIC. [23]. If reliable amplitude estimation is possible, the hard-decision detectors generally out-perform their simpler soft-decision counterparts. This thesis makes use of a hyperbolic-tangent-based algorithm of soft-decision detection that performs better than the hard-decision detectors. This soft-decision algorithm is explained in detail in chapter 5 of the thesis.

The most important of these detectors are discussed below:

3.3.3.1 Successive Interference Cancellers (SIC)

The SIC detector takes a serial approach to canceling interference. Each stage of this detector's decisions regenerates and cancels out one additional user from the received signal so that the remaining users see less MAI in the next stage. [23] Since the strongest signal has the most negative effect, it is important to cancel the strongest signal in each stage before detection of other signals [22]. The reason for canceling the signals in descending order of signal strength is:

- It is easiest to achieve acquisition and demodulation on the strongest users and hence provides the best chance for correct data decisions

- The removal of the strongest user gives the most benefit for the remaining users

The result of this algorithm is that the strongest user will not benefit from any MAI reduction while the weakest users will potentially see a huge reduction in their MAI.

The SIC detector has the potential to provide significant improvement over the conventional detector. However, for every cancellation stage, a bit of delay is required. Hence, a trade-off must be made between the number of users that are cancelled and the amount of delay that can be tolerated. There is also a need to reorder signals whenever the power profile changes. Hence, a trade-off must also be made between the precision of the power-ordering and the acceptable processing complexity. A potential problem with the SIC detector occurs if the initial data estimates are not reliable. If the bit estimate is wrong, the interfering effect of that bit on the signal-to-noise ratio is quadrupled in power. [23]

3.3.3.2 Parallel Interference Cancellers (PIC)

In contrast to the SIC detector, the PIC detector estimates and subtracts out all of the MAI for each user in parallel. The initial bit estimates are derived from the first stage, called stage 0, of the detector which may be e.g. a matched filter detector. These bits are then used to produce a delayed estimate of the received signal for each user. A partial summer sums up all but one input signal at each of its outputs, which forms the complete MAI estimate for each user. In this way, the MAI for each of the user is generated in parallel and subtracted out simultaneously from all the users in a single stage. In this thesis, different types of PIC detectors have been utilized in the receiver.

The process can be repeated for multiple stages. Each stage takes as its input the data estimates of the previous stage and produces a new set of estimates at its output. Perfect data estimates, coupled with our assumption of perfect amplitude and delay estimation result in the complete elimination of MAI. [23]

PIC detectors are classified into the following two types:

- **Linear PIC (LPIC)**

LPIC generates MAI estimates using the soft values of the decision statistics from the previous stage. There is significant interest in LPIC due to its simplicity in implementation, analytical tractability, and good performance under certain specific conditions [27] (discussed in detail in [28], [29], [30]).

A more recently proposed LPIC detector makes use of soft tentative decisions from the previous stage to estimate and subtract the MAI from the current stages as in normal LPIC, but in the final stage a hard decision device is used.

Unlike HDPIC, the LPIC does not need to know the user amplitudes since the soft stage outputs are used as estimates for the product of each user's bit and amplitude. Furthermore, since the LPIC does not form a hard decision until the last stage, the LPIC detector does not inherently possess the interference doubling problems found in the HDPIC detector. [28]

- **Hard-Decision PIC (HDPIC)**

The basic idea behind HDPIC is to remove the MAI unconditionally [20]. Each stage generates an output of tentative hard bit decisions for each user. Using the tentative hard bit decisions from the prior stage, the next stage generates its MAI estimates by multiplying these tentative decisions by the corresponding user amplitudes, and appropriate cross-correlation factors (in the case of CDMA). These MAI estimates are then subtracted from the original observation and the result is passed through a hard decision device to form new tentative hard decisions for the next stage.

If the multistage detector has perfect knowledge of the user amplitudes and any cross correlation factors, and if the prior stage's bit decisions are all correct, then the MAI can be perfectly cancelled and single-user performance is achieved at that stage. However, if the prior stage's output leads to a bit decision error, then the subtraction of this MAI from the original observation will result in doubling of interference on the user's decision statistics.

Although such an interference cancellation is not optimal in all cases, it is the best way of PIC detection when the difference between the carrier frequency offsets of different users is high [28]. A comparison between the performance of HDPIC and

LPIC is presented in [28], where based on a comparison between the mean-square error (MSE) of the MAI estimators, it has been shown that HDPIC provides a superior MAI estimation than LPIC. [27]

3.3.4 COMPARISON OF SIC AND PIC

A comparison between SIC and PIC detectors yield that:

- The SIC detector performs better than the PIC detector in a fading environment affected by a near/far power-control problem. However, in a well-power-controlled environment the PIC detector performs better than the SIC detector. [31]
- The PIC detector requires more hardware, but the SIC detector faces the problem of power re-ordering and large delays. [23]

CHAPTER 4

RELEVANT TECHNICAL WORK

4.1 RELATED WORK

The transmission of DVB-T signals makes use of COFDM in the form of a Single Frequency Network. Such SFNs constitute a number of base stations that transmit the same data simultaneously and, in effect, form a channel with long delay spreads. The signals from each of the base stations are superimposed on each other and received by the receiver where the signals are interpreted as useful or interfering signals based on the receiver implementation method. A simulation of such a SFN scenario has been conducted in [32] where the performance of the network in terms of SINR has been investigated along different network parameters such as inter-site distance, base station heights and the length of the cyclic prefix.

Channels with long delay spreads such as the SFN in [32] can be improved upon via the use of equalization and detector techniques in the receiver. The authors in [33] implement a conventional DVB-T broadcast system without any additional equalization and make a comparison with the ATSC broadcast system. In [16] a single-tap MMSE-DFE equalizer is implemented over a bandwidth-efficient OFDM system. This bandwidth-efficient OFDM system does not make use of the guard interval and allows ISI and ICI components to enter the data samples. It uses sufficient statistics in channel equalization via the implementation of a single-tap DFE and on comparison with a conventional OFDM system shows that the bandwidth-efficient system performs better.

In [34], the author implements a DFE-based receiver for OFDM systems having channels with long delay spreads such as for DVB-T. The length of the cyclic prefix is not increased in the long delay spread channel, and in order to compensate for this, DFE is implemented in the receiver to preserve system efficiency. The paper demonstrates that the channel impairment caused by the long delay spreads can be overcome by such an arrangement and without the requirement of an increase in CP.

The DFE utilizes a feed-forward filter that caters to ICI and noise components in the signal and a feed-back filter that eliminates the ISI based on previous symbol decisions. Utilizing a conventional feed-forward filter such as the MMSE being implemented in [16] has the disadvantage of computing the inverse of the channel correlation matrix. The computation of the inversion of such a matrix, especially in the case of channels with long delay spreads, proves to be difficult to perform in real time.

In order to make the DFE more efficient and the receiver computation less complex, this thesis makes use of the PIC detector as the feed-forward filter for the DFE. Different kinds of multi-user detectors are discussed and compared in detail with each other in [23] and [22]. These papers discuss multi-user detection schemes in the context of uplink DS-CDMA. A comparison between different methods of SIC and PIC detetors has been presented in [22] in terms of the average BER vs. the number of users. A comparison between the performance of HDPIC and LPIC is presented in [28], where based on a comparison between the mean-square error (MSE) of the MAI estimators, it has been shown that HDPIC provides a superior MAI estimator than LPIC [27].

An advanced equalized PIC (EPIC) receiver that equalizes the data estimates of the previous two stages is proposed in [35]. The work has been presented for MC-CDMA systems in downlink transmissions and shows that the proposed EPIC receiver significantly improves the system performance.

HDPIC for uplink OFDMA is presented in [20]. A decrease in bit error rates has been shown with the implementation of HDPIC as compared to performance without any interference canceller.

4.2 APPLICATION OF MULTI-USER DETECTION

Most of the work done along the application of multi-user detectors has been done in uplink transmission for mobile networks. This is due to the fact that uplink traffic consists of asynchronous transmission of signals from different users when they transmit to the base station. In the case of OFDMA, different users transmitting simultaneously may have a carrier frequency offset which causes a loss in orthogonality between the sub-carriers. In the case of DS-CDMA, the near/far problem requires tight power-control and attendant complexity which can be catered for much easily by the use of multi-user detection.

In downlink transmission, all users experience the same carrier frequency offset since only the base station transmits to all the users. So the orthogonality of each sub-carrier with the others is not lost. Similarly the issue of power-control is of no consequence because the base station transmissions are at a controlled power-level. In a conventional wireless system, due to these reasons, research along multi-user detection is usually confined to uplink only.

However, multi-user detection can also be used to improve the performance of the receiver in channels with long delay spreads, such as in the case of DVB-T application. The marked performance gain of such detectors is desired in a SFN scenario where the channel consists of long delay spreads due to which performance of the conventional receiver is compromised. Multi-user detection offers a promising solution to yield better performance in such conditions.

In context to this thesis, a PIC multi-user detector has been implemented within a DFE structure to improve performance in channels with a long delay spreads. It is worth mentioning here that the PIC detector has been used for multi-channel detection, removing ICI, rather than multi-user detection, removing MAI. Since the application is based on DVB-T networks, there is an absence of multiple users. A number of TV channels replace the users. The underlying theory and principle of implementation remains the same.

CHAPTER 5

SIMULATION WORK

5.1 IMPLEMENTATION OF THE SIMULATOR

The focus of this thesis' simulation work is to implement a receiver with a DFE-PIC equalization scheme. The receiver is aimed to be used in channels with long delay spreads. SFN channels that are a part of the DVB-T transmission networks are an example of such channels and have been utilized in this thesis in order to measure the gain in performance achieved with such receivers. Matlab^{TM} 7.1 has been employed in order to develop the simulator.

The mentioned DVB-T transmission systems are based on OFDM and as such, the simulation work has been developed with OFDM symbol transmissions. QPSK modulation has been used to generate the OFDM symbols. The Rayleigh channel model with additive white Gaussian noise (AWGN) has been implemented for signal transmission.

The worst-case scenarios of such channels with long delay-spreads have been simulated and the power-delay profiles (PDP) of such cases have been generated within the context of this thesis simulation. Additionally, simulated SFN channels are also used in this thesis, which have been imported from the simulated work of [32]. The results are finally displayed in the form of BER versus SNR curves which are used to observe and analyze any performance improvement in each of the scenarios implemented.

5.2 RECEIVER DESIGN

The design of the proposed receiver realizes a DFE-PIC configuration. The PIC detector is used as the feed-forward filter in order to remove ICI components in the received signal. ISI components are removed through the use of the feed-back filter of the DFE. The basic block diagram of such a DFE receiver is shown in figure 5.1.

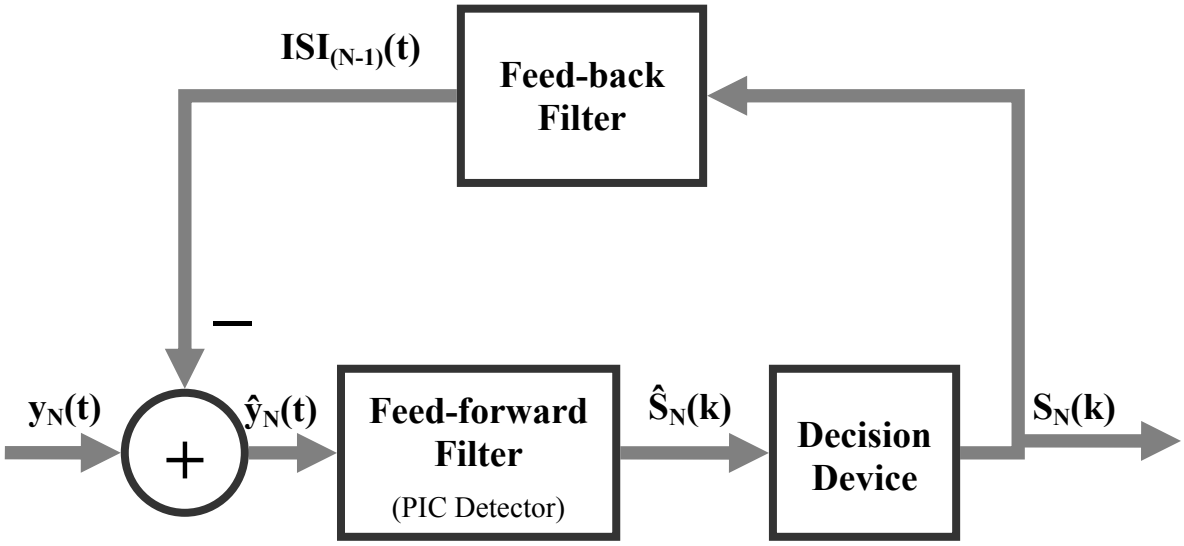

Figure 5.1: Block Diagram of DFE-PIC Receiver

The implementation of the feed-forward PIC detector is done in two steps. The initial stage, termed as stage 0 of the detector, determines the post-FFT observation by taking the Fourier transform of the received signal. The symbols are extracted from the post-FFT observation without any removal of ICI.

In the second step, the latter stages of the PIC detector are iterated by using the estimated symbol from previous stages to estimate the ICI for the current stage. This ICI is deducted from the post-FFT observation of stage 0 and the symbol is again estimated for the current stage.

A basic block diagram of the PIC detector is shown in figure 5.2.

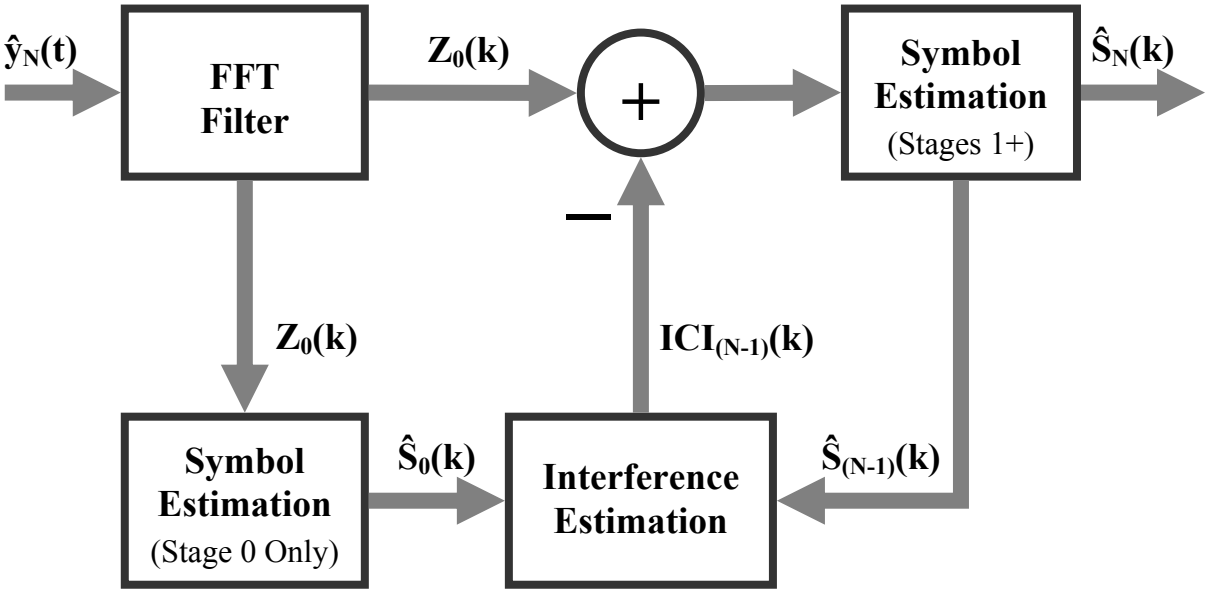

Figure 5.2: Block Diagram of the PIC Detector

Interference estimation is derived based on the ICI components present in the received signal and the estimates of the symbol from the previous PIC stages. With perfect channel estimation, ICI can be completely removed from the received signal and symbols can be accurately extracted. As the PIC stages iterate forward, the estimate of the ICI gets more and more accurate. In this way the PIC stages, beyond stage 0, estimate and subtract out all the ICI in each channel in parallel.

Depending upon the simulation scenario, the decision device may utilize a hard and/or a soft decision. The final estimated symbol that results from the PIC detector and the decision device is looped back through the feed-back filter. The feed-back filter extracts the ISI components of this symbol and removes these ISI components from the next incoming symbol. In this way the DFE works with the feed-back filter removing the ISI components while the feed-forward filter removing the ICI components.

Channel estimation is utilized in order to formulate the ISI and ICI components. The channel can be estimated by the regular transmission of pilot signals through the channel. However, within the context of this thesis work, perfect knowledge of the channel has been assumed.

5.2.1 MATHEMATICAL REALIZATION OF THE PROPOSED RECEIVER

Considering $y_N(t)$ as the time domain signal received at the receiver input and I_{ISI} as the ISI components derived from channel estimation and OFDM symbol characteristics, the feed-back step of DFE implementation is given by equation 5.1.

$$\hat{y}_N(t) = y_N(t) - I_{ISI}\hat{X}_{(N-1)}(t) \tag{5.1}$$

In this feed-back step, the ISI components in the received signal are removed based on the estimated previous symbol from the PIC detector and the decision device. The previous symbol is converted to time domain using inverse fast Fourier transform (IFFT) and the ISI cancellation is also done in time domain from the received signal. In equation 5.1, $\hat{X}_{(N-1)}(t)$ represents the previously estimated symbol in time-domain arriving from the feed-back filter.

In the feed-forward step of DFE, the resulting time-domain signal $\hat{y}_N(t)$ is processed by the PIC detector and goes through the decision device to get symbol estimation for the current symbol. Neglecting noise, this signal $\hat{y}_N(t)$ is composed of the current transmitted symbol along with ICI components and the channel correlation matrix. The channel correlation matrix consists of the channel taps required to recover the actual transmitted symbol.

Considering the actual transmitted symbol as $X_N(t)$, the ICI components as I_{ICI} and the channel correlation matrix as $\bar{H}$, equation 5.2 details the received signal components at the input of the PIC detector.

$$\hat{y}_N(t) = \bar{H}X_N(t) - I_{ICI}X_N(t) \tag{5.2}$$

In stage 0 of the PIC detector, this received signal undergoes fast Fourier transform (FFT) to convert the signal to frequency domain components. The resulting signal Z_0 is termed as the post-FFT observation for the PIC detector, based on which all symbol estimation is done.

Taking the Fourier transform, the channel correlation matrix converts to λ, which is a diagonal matrix composed of the required number of channel taps for correct symbol recovery. The inverse of this diagonal matrix is much simpler to compute in

the receiver as compared to the channel correlation matrix. This is the reason why the PIC detector is more practical than a decorrelating or MLSE detector.

The result of the Fourier transformation is shown in equation 5.3 displaying the components of the post-FFT observation Z_0.

$$Z_0 = \lambda S_N(k) + FI_{ICI}\overline{F}S_N(k) \tag{5.3}$$

In equation 5.3, $S_N(k)$ represents the actual transmitted symbol in frequency domain while $FI_{ICI}\overline{F}$ represents interference components. Here, F and $\overline{F}$ represent Fourier transform (FFT) and inverse Fourier transform (IFFT) functions respectively.

Following the derivation of the post-FFT observation in stage 0, the symbol is estimated without removing any ICI components in this stage. This is done using the inverse of the diagonal channel matrix λ on the initial observation. This step is shown in equation 5.4.

$$\hat{S}_0(k) = \lambda^{-1}Z_0 \tag{5.4}$$

This estimated symbol $\hat{S}_0(k)$ from stage 0 is used to calculate the ICI estimate in the next stage of the PIC detector. The ICI estimate is removed from the post-FFT observation Z_0 to get a new estimate at the end of the stage. For any stage of the PIC detector, after stage 0, the same process is repeated. The previous stage' symbol estimate is used to calculate the ICI estimate and remove this ICI from the post-FFT observation to get a new symbol estimate. A general solution depicting this process for the m^{th} PIC stages is shown in equations 5.5 and 5.6

$$Z_m = Z_0 - FI_{ICI}\overline{F}S_{(m-1)}(k) \tag{5.5}$$

$$\hat{S}_m(k) = \lambda^{-1}\hat{Z}_m \tag{5.6}$$

The estimated symbol of the final PIC stage goes through a decision device which maps it according to the original symbol amplitudes and phases. This final output of the feed-forward filter is the output of the receiver and is also fed back to the feed-back filter for ISI removal from the next incoming symbols.

5.3 RECEIVER COMPLEXITY

The additional complexity of the proposed receiver in comparison to the conventional OFDM receiver is described below:

- DFE Feed-back Loop: This loop requires the implementation of IFFT over the estimated symbol and then multiplication of the result with ISI components from the channel estimation. Finally, estimated symbol's ISI is subtracted from the received symbol.

  Implementation of the IFFT requires $N_{FFT}xN_{FFT}$ multiplications and $N_{FFT}(N_{FFT}-1)$ additions. The same calculations are required for ISI estimation. ISI elimination from the received signal requires N_{FFT} additions. Therefore the DFE feed-back loop requires $2xN_{FFT}^2$ multiplications and $(2xN_{FFT}^2 - N_{FFT})$ additions.

- PIC Detector: The PIC detector requires inversion of a diagonal channel matrix once. Symbol estimation requires multiplication of a diagonal matrix with received signals. Interference estimation requires a further multiplication while summing is required to remove ICI components in each stage.

  This relates to N_{FFT} divisions for channel matrix inversion in stage 0. Stage 0 also utilizes symbol estimation which requires N_{FFT} multiplications. Each additional PIC stage requires interference estimation with $N_{FFT}xN_{FFT}$ multiplications and $N_{FFT}(N_{FFT}-1)$ additions and an additional symbol estimation. ICI elimination requires N_{FFT} additions. Therefore stage 0 requires N_{FFT} divisions and N_{FFT} multiplications. Each PIC stage requires $(N_{FFT}^2 + N_{FFT})$ multiplications and N_{FFT}^2 additions.

Hence the overall additional computations required by the DFE-PIC receiver over the conventional OFDM receiver are N_{FFT} divisions, $(3xN_{FFT}^2 + 2xN_{FFT})$ multiplications and $(3xN_{FFT}^2 - N_{FFT})$ additions for PIC detector with one stage.

5.4 SIMULATION PARAMETERS AND VARIABLES

5.4.1 OFDM SYMBOL PARAMETERS

The OFDM parameters utilized in the simulation are listed in table 5.1.

Parameters	Value
System Bandwidth	1.25 MHz
Number of Sub-Carriers	128
Sub-Carrier Separation	9.766 kHz
OFDM Symbol Period	102.4 μ
Number of Cyclic Prefix	32

Table 5.1: OFDM Symbol Parameters

5.4.2 FFT SIZE

The size of the FFT used in the simulation work is 128. The Matlab functions of 'fft' and 'ifft' have been utilized for conversion between frequency and time domain of the signals. The discrete Fourier transform is defined by the formula:

$$X_K = \sum_{n=0}^{N-1} x_n e^{-\frac{2\pi i}{N} nk} \tag{5.7}$$

In equation 5.7, X_K is the frequency domain signal being calculated while x_n is the time domain signal being analyzed. Here, N is the number of FFT points and the indices n and k run from 0 to (N-1). [36]

5.4.3 TOTAL NUMBER OF SYMBOLS IN ONE OFDM SYMBOLS

The number of symbols incorporated in one OFDM symbol has been kept equal to the FFT size, i.e. 128. Test cases have also been run with varying symbols lengths, however, all results displayed in this thesis report have been simulated with 128 symbols.

5.4.4 MODULATION SCHEME

Gray-coded QPSK modulation has been implemented in order to generate the transmitted OFDM symbols.

5.4.5 NUMBER OF CHANNEL TAPS

A maximum of 128 channel taps, equal to the FFT size, have been implemented in order to simulate the long delay-spread channel. The simulation is capable of running a maximum of $N_{maxtaps}$ channel taps, which is the extent of taps a single-tap DFE equalizer can cover. This is illustrated in equation 5.8.

$$N_{\max taps} = 2 \times CP + N_{FFT} \tag{5.8}$$

5.4.6 CHANNEL REALIZATION

The Rayleigh channel model is implemented in this simulation. To this end, normally-distributed random channel taps are generated in each of the iterations which are scaled to the power-delay profile (PDP).

5.4.7 NOISE MODEL

Additive White Gaussian Noise (AWGN) has been incorporated into the channel. This has been introduced through the generation of normally-distributed random noise values that are scaled according to the SNR values. Within each SNR loop, the channel is implemented numerous times in order to achieve an AWGN model.

5.1.1 ITERATIONS

Four loops have been incorporated in the simulation work:

- The SNR loop runs within the range of 1 to 24 dB with a total of 9 iterations. Each iteration runs a new value of SNR based on which the receiver is analyzed
- Within each SNR iteration, 500 iterations of different channel realizations are implemented. Normally-distributed random channel taps are generated for each realization
- Each channel realization incorporates a maximum of 6 iterations for the ISI-removal loop. However, each iteration implements over a new symbol and presents the error-propagation problem of the DFE feed-back loop
- Within each ISI-removal loop, the PIC detector is implemented in the form of a loop too. Each iteration of the loop represents a new stage of the detector and a maximum of 6 stages have been used

5.4.8 ICI SCALING FACTOR

This thesis implements the PIC detector in order to remove ICI components. As such, each stage of the PIC detector estimates ICI components based on the previous stage symbol estimate and the channel estimation. With each new PIC stage, the ICI estimate becomes more and more accurate.

In various scenarios, it may sometimes become necessary to remove the ICI partially only in a stage. This may be due to inaccuracy in channel estimation or as part of a configuration of the detector. In order to limit error propagation due to inaccurate ICI estimation, the detector may be configured in such a way that a lesser percentage of ICI is removed in each stage. This allows the detector to provide better performance in case of huge errors in the channel estimate. The ICI scaling parameter realizes the scaling factor of the ICI that is removed in each stage of the PIC detector.

5.4.9 SOFT DECISION SCALING FACTOR

The scaling factor of a soft-decision device represents the magnitude to which the decision will match an actual symbol value. Based on the detector's confidence of the estimated symbol, the scaling factor will shift the received values towards the actual values proportionally. The greater the scaling factor value, the more the soft decision device behaves like a hard decision device. A hyperbolic tangent function has been utilized to represent the soft-decision process and the effect of the scaling factor is displayed in equation 5.9, where 'factor' is the soft-decision scaling factor:

$$soft\_dec = \tanh(factor \times \hat{S}_N(k)) \tag{5.9}$$

5.5 SIMULATOR FLOW CHART

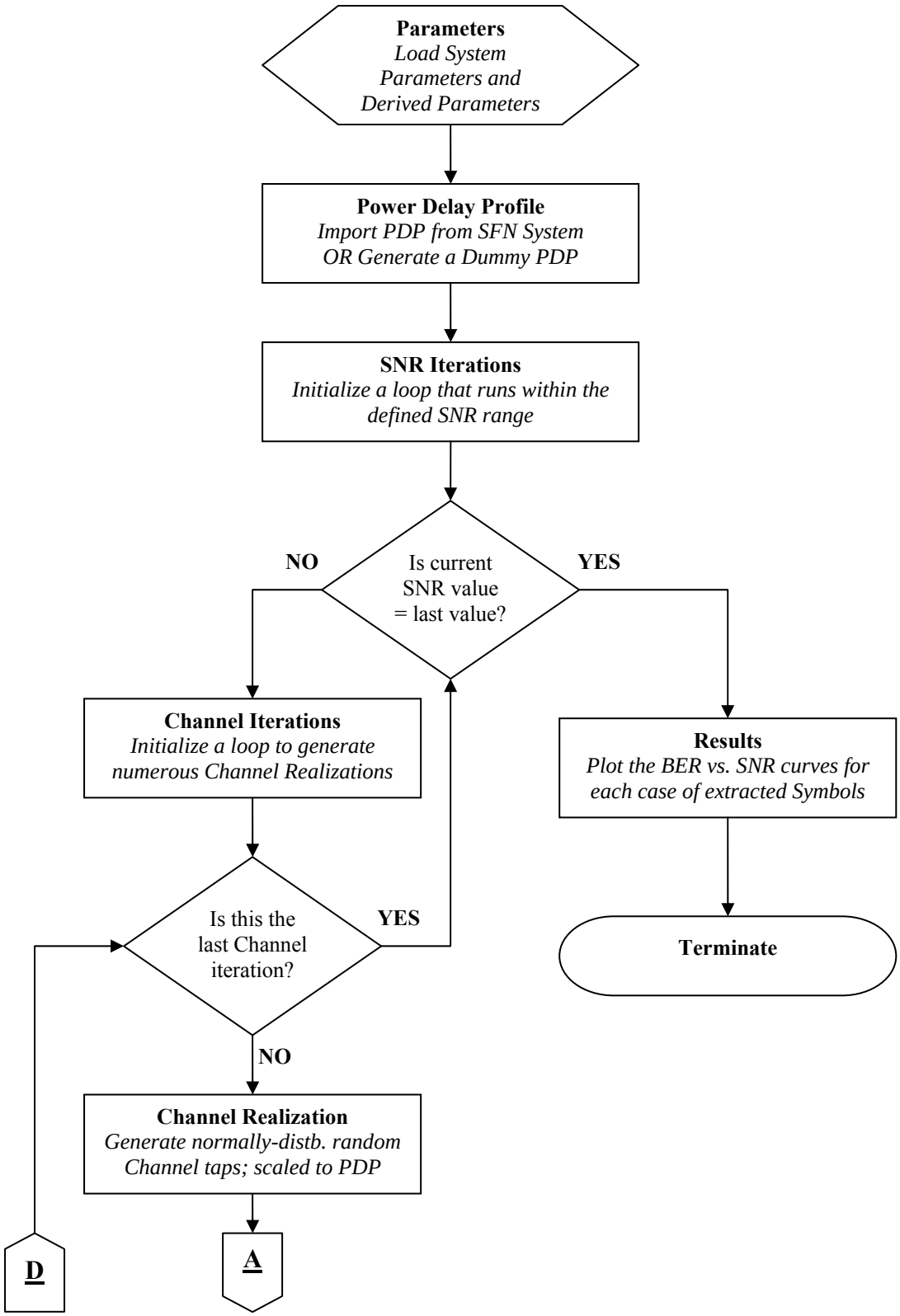

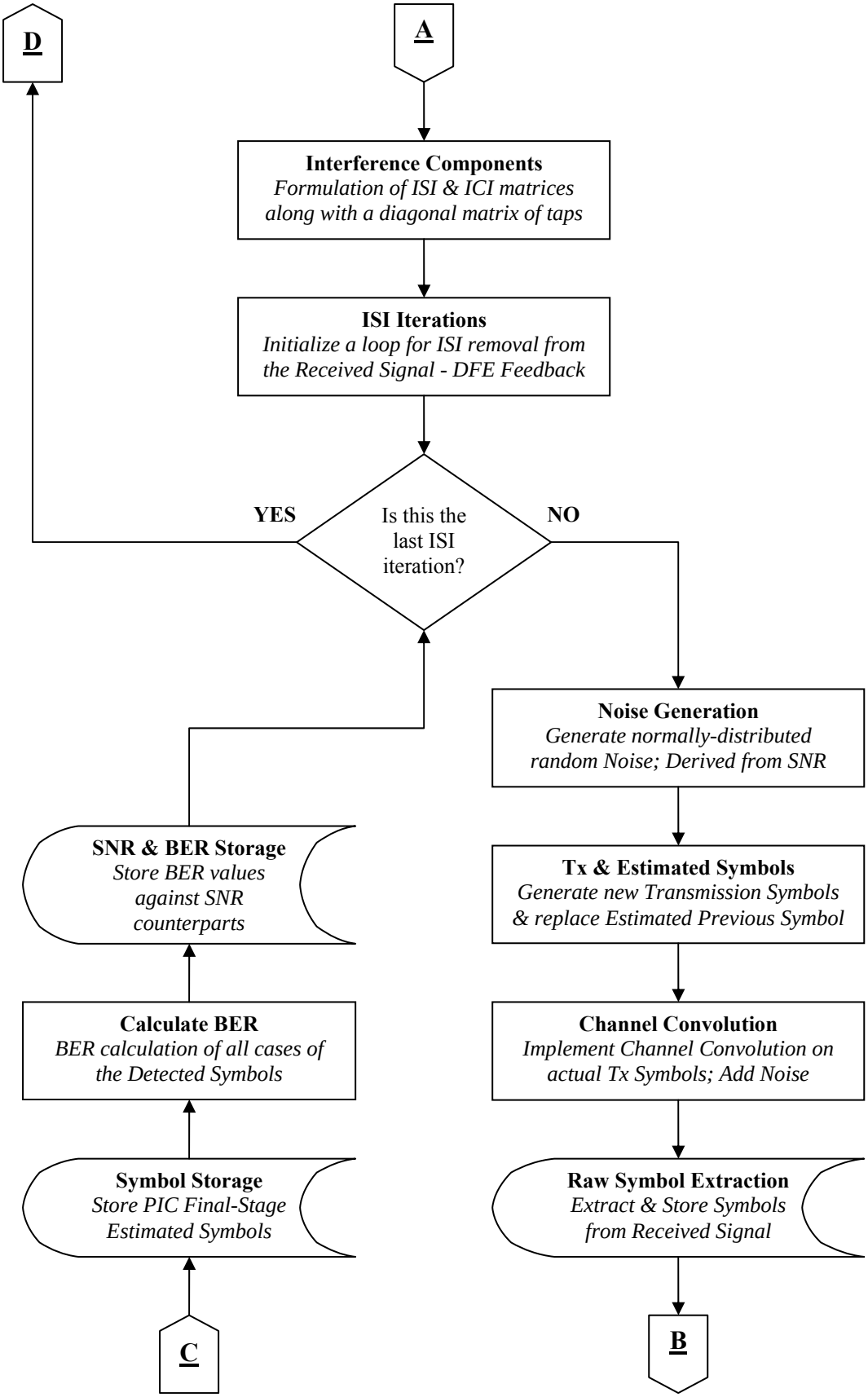
D
A
Interference Components
Formulation of ISI & ICI matrices along with a diagonal matrix of taps
ISI Iterations
Initialize a loop for ISI removal from the Received Signal - DFE Feedback
YES
Is this the last ISI iteration?
NO
Noise Generation
Generate normally-distributed random Noise; Derived from SNR
SNR & BER Storage
Store BER values against SNR counterparts
Tx & Estimated Symbols
Generate new Transmission Symbols & replace Estimated Previous Symbol
Calculate BER
BER calculation of all cases of the Detected Symbols
Channel Convolution
Implement Channel Convolution on actual Tx Symbols; Add Noise
Symbol Storage
Store PIC Final-Stage Estimated Symbols
Raw Symbol Extraction
Extract & Store Symbols from Received Signal
C
B

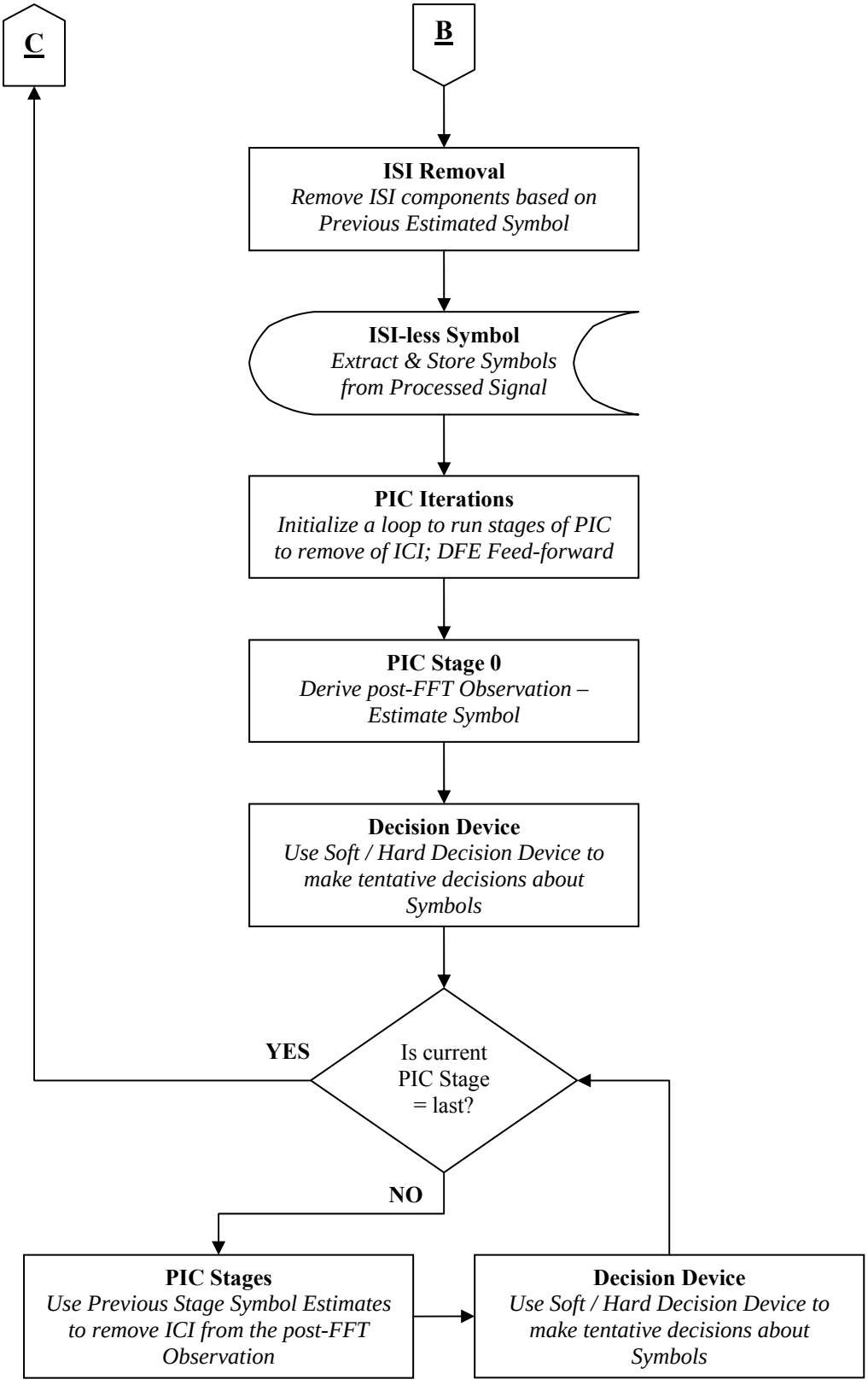
C
B
ISI Removal
Remove ISI components based on Previous Estimated Symbol
ISI-less Symbol
Extract & Store Symbols from Processed Signal
PIC Iterations
Initialize a loop to run stages of PIC to remove of ICI; DFE Feed-forward
PIC Stage 0
Derive post-FFT Observation – Estimate Symbol
Decision Device
Use Soft / Hard Decision Device to make tentative decisions about Symbols
YES
Is current PIC Stage = last?
NO
PIC Stages
Use Previous Stage Symbol Estimates to remove ICI from the post-FFT Observation
Decision Device
Use Soft / Hard Decision Device to make tentative decisions about Symbols

5.6 SIMULATION STEPS

The simulation has been implemented in the following steps:

- Load system parameters
- Generate a random PDP or import a PDP from the SFN simulation
- Initialize and start SNR loop iterations
    - Realize SNR value
    - Initialize and start channel iterations
        - Generate Rayleigh channel taps - scaled to PDP
        - Formulate ISI and ICI components based on channel taps
        - Initialize and start ISI-removal iterations (DFE feed-back)
            - Generate AWG noise based on SNR value
            - Replace previous symbol with next estimated previous symbol
            - Generate new current symbol
            - Implement channel convolution on actual transmitted symbols (previous and current) and add noise.
            - Extract and store symbol estimates from the received signal (Conventional Receiver)
            - Remove ISI components (based on estimated previous symbol) from the received signal
            - Extract and store symbol estimates from the ISI-processed signal
            - Implement PIC stage 0; derive post-FFT observation and estimate symbols without ICI removal
            - Implement Soft/Hard decision
            - Initialize and start PIC stage iterations (DFE feed-forward)
                - Use previous stage's symbol estimate to remove ICI from post-FFT observation
                - Implement Soft/Hard decision
            - Extract and store symbol estimates from the PIC processed signal
            - Calculate and store BER values against respective SNR values
- Plot the BER vs. SNR curves for each case of the extracted symbols

CHAPTER 6

RESULTS AND ANALYSIS

6.1 NUMBER OF PIC STAGES

This thesis implements the PIC detector as the feed-forward filter of the DFE in the receiver. In this configuration, the PIC detector is used to remove the ICI components in the signal being processed through the equalizer. The ICI components in the signal depend upon the channel characteristics and the symbol being processed.

The initial stage, termed as stage 0, does not remove any ICI and produces the post-FFT observation and the initial symbol estimate. The latter stages utilize the symbol estimates from the previous stages to estimate ICI for each stage. This ICI is deducted from the post-FFT observation of stage 0 to produce symbol estimates for the current stage of PIC.

It is important to realize that if the ISI components are still present in the signals that enter the PIC detector, each stage of the detector will formulate incorrect ICI estimates. These incorrect ICI estimates cause symbol estimation errors at each PIC stage and as the number of stages grow, the error rate increases proportionally. The reason being, that this thesis utilizes the PIC detector only to remove the ICI components. The PIC detector is not designed here to remove any additional ISI components, which are already being taken care of by the DFE feed-back loop. A such, any ISI present in the PIC stages causes errors in the symbol estimations that cannot be handled by the PIC.

In order to analyze how the receiver reacts to an increase in PIC stages, the current scenario implements three different cases with varying number of stages in each case. The results of these simulations are shown in figures 6.1 to 6.4 where an improvement in BER is analyzed against an increase in SNR for each of the cases. Table 6.1 shows the parameters and variables used in the simulation of these cases.

FFT Size (N_{fft})	128
Channel Taps (N_{taps})	128
No. of Symbols in OFDM Symbol (N_{sym})	128
Cyclic Prefix length (CP)	32
SNR Range	1:24 dB
Channel Realizations (N_{drops})	500
ISI Iterations (N_{isi})	6
PIC Stages (N_{pic})	2 4 6
Decision Device	Hard Decisions
ICI Scaling Factor	100 %
Soft Decision Scaling Factor	N/A

Table 6.1: Parameters/Variables implemented in PIC Stage Scenario

Figures 6.1, 6.2 and 6.3 show the response of the receiver, when the number of PIC stages are 2, 4 and 6 respectively. The figures display the performance level of the FFT receiver, which is the conventional OFDM receiver, and used as a reference level in order to measure the performance of other receiver configurations. Compared to the conventional receiver, the performance of DFE only, PIC only and the DFE-PIC receivers are gauged in each of the figures. Furthermore, figure 6.4 compares the PIC only and the DFE-PIC receiver performance for each of the cases discussed.

As the stages increase, the ICI estimate gets better and the performance of the DFE-PIC receiver improves slightly. However, if ISI components are still present in the PIC stages, as in the PIC only receiver, then with each increasing stage, the

performance of the PIC detector gets worse and the symbol estimation deteriorates rather than showing improvement.

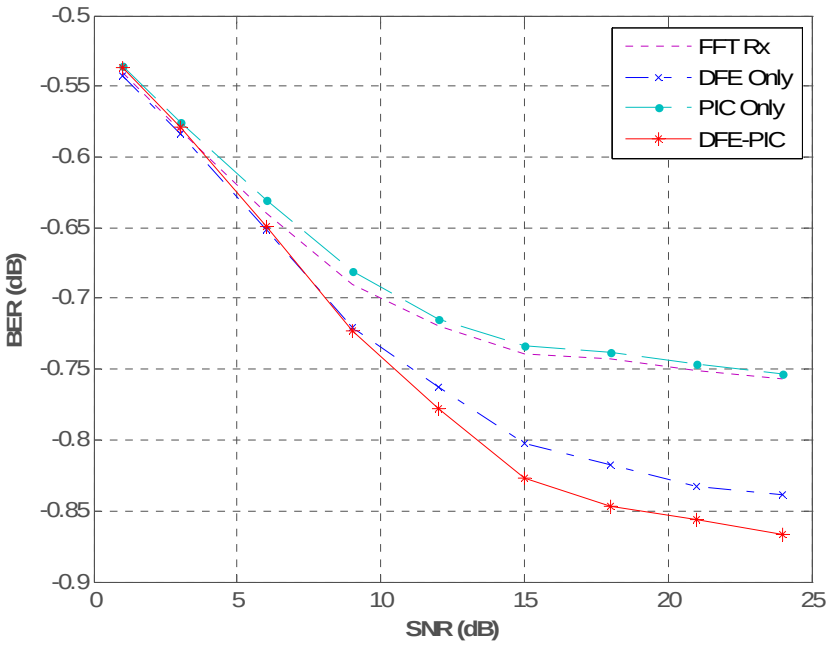

Figure 6.1: Receiver Performance with 2 PIC Stages

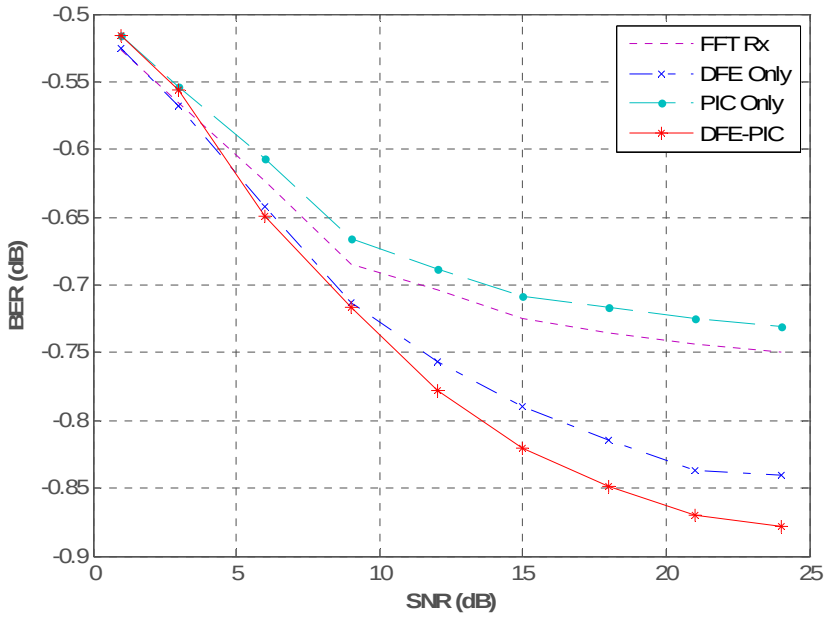

Figure 6.2: Receiver Performance with 4 PIC Stages

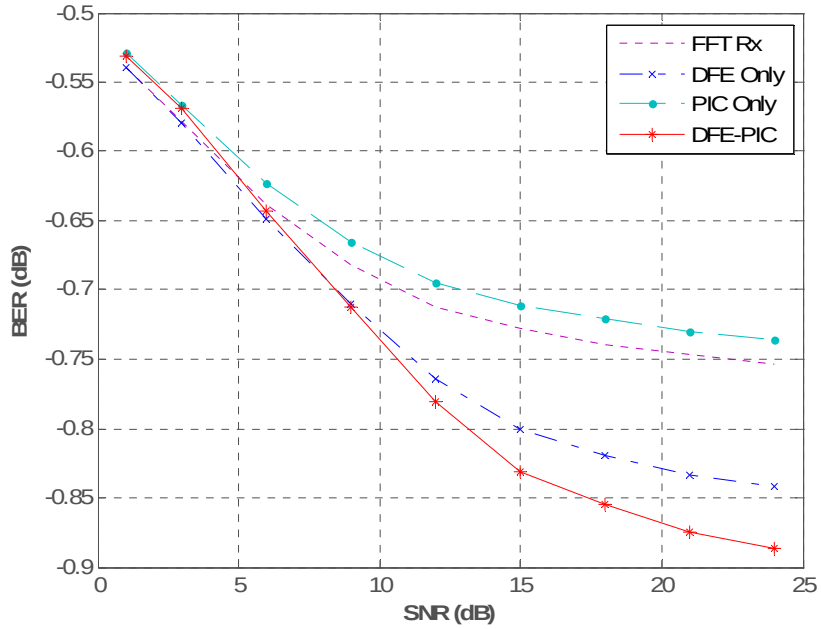

Figure 6.3: Receiver Performance with 6 PIC Stages

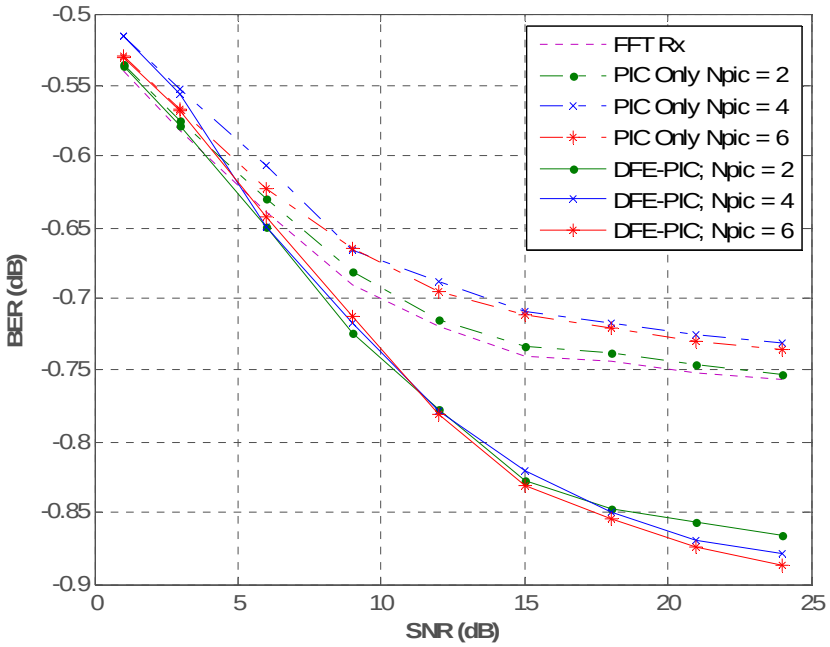

Figure 6.4: Performance Comparison of Effect of PIC Stages

Figure 6.4 shows a comparison of PIC-only and DFE-PIC curves of the three different cases. As the number of stages increase, the DFE-PIC symbol estimation improves, just as expected. However, the PIC-only BER performance is always worse even than

that of the received signal curve. This is because, as explained above, the additional ISI causes incorrect ICI estimation which gets greater with each iteration of PIC stage. With an increase in stages, the PIC-only symbol estimation deteriorates. It is clear that the PIC-only detector is not useful in our current receiver configuration since it makes the symbol estimation worse.

6.2 ERROR PROPAGATION DUE TO DFE FEEDBACK

ISI cancellation takes place in the feed-back loop of the DFE. The previously processed symbol is routed back to the incoming signal at the receiver and based on the channel characteristics, the ISI components from the previous symbol are calculated and cancelled out of the received signal.

Here, it is important to realize that every time a new channel realization is simulated, the first iteration of the DFE runs without any previous symbols and thus contains no ISI at all. As the iterations increase, previous symbols introduce ISI into the received signals. An error in the current symbol estimate causes increased number of errors into the next iteration's symbol estimation. In this way the errors propagate as the number of iterations is increased.

In order to analyze how these errors propagate, the current scenario observes how the DFE-PIC receiver reacts to an increase in ISI iterations. The results of these simulations are shown in figures 6.5 and 6.6 displaying a comparison between three different cases with a varying number of ISI iterations. Improvement in BER is analyzed against an increase in SNR for each of the cases. Furthermore, table 6.1 shows the parameters and variables used in the simulation of these cases.

Figure 6.5 displays how the detector reacts at the first ISI iteration. In this case, the absence of a previous symbol means there are no ISI components present in the received signal. The absence of ISI allows for better ICI estimation. Hence we observe that the DFE-only BER conforms to the performance of the received signals' BER curve. Similarly the lack of ISI ensures that the PIC-only BER conforms to the performance of the DFE-PIC BER curve. Eventually we observe a marked BER improvement of 0.2 dB between the DFE-only and DFE-PIC curves.

FFT Size (N_{fft})	128
Channel Taps (N_{taps})	128
No. of Symbols in OFDM Symbol (N_{sym})	128
Cyclic Prefix length (CP)	32
SNR Range	1:24 dB
Channel Realizations (N_{drops})	500
ISI Iterations (N_{isi})	1 3 6
PIC Stages (N_{pic})	4
Decision Device	Hard Decisions
ICI Scaling Factor	100 %
Soft Decision Scaling Factor	N/A

Table 6.2: Parameters/Variables implemented in Feedback Error Scenario

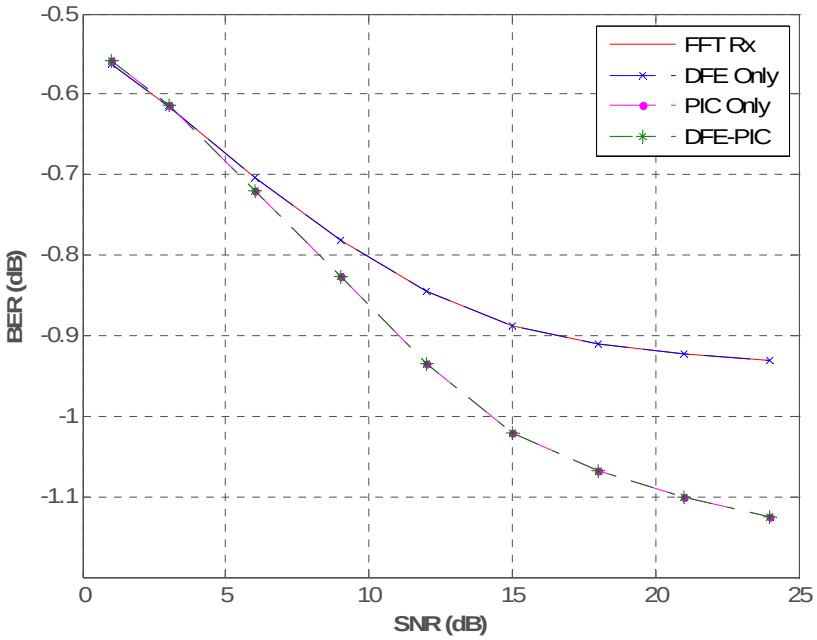

Figure 6.5: Receiver Performance at 1st ISI Iteration

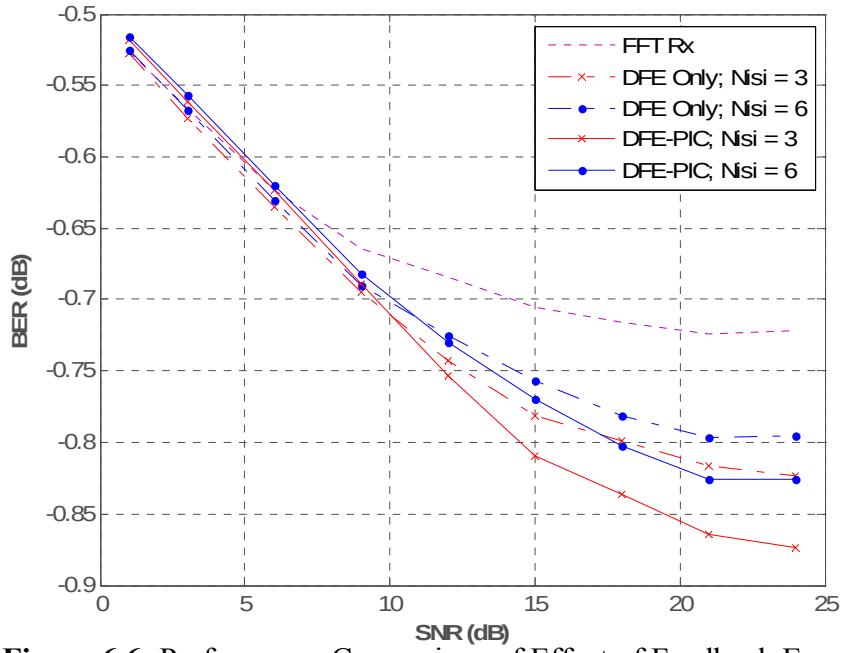

Figure 6.6: Performance Comparison of Effect of Feedback Error

Performance comparison between ISI iterations of 3 and 6 is shown in figure 6.6. The figure displays how increasing the ISI iterations affects the BER performance of the DFE-only and the DFE-PIC receivers. As the iterations increase, the BER performance deteriorates. The DFE-only and the DFE-PIC BER deteriorate by approximately 0.025 dB and 0.05 dB respectively, as the iterations increase from 3 to 6. The results comply with the reasoning discussed earlier in this scenario. Detector decision errors propagate through to the next iterations where they cause an increase in errors in the following decisions.

6.3 ICI SCALING FACTOR

The proposed receiver implements a PIC detector in order to remove the ICI components in the feed-forward of DFE. The ICI estimation for each PIC stage is done based on the channel characteristics and the symbol estimate from the previous PIC stage. An error in symbol estimation of one PIC stage, doubles in the next stage, specially in the case of hard decisions taken on symbol estimates. However, such error propagation can be limited and controlled by decreasing the effect of ICI on the symbol estimation of each stage. This is achieved through scaling of the ICI estimate.

The current scenario deals with the reaction of the DFE-PIC to a variation in the ICI estimation scaling. Four different cases are implemented with a varying degree of ICI

scaling factors. The results of these simulations are shown in figure 6.7 where an improvement in BER is analyzed against an increase in SNR for each of the cases. Table 6.3 shows the parameters and variables used in the simulation of these cases.

FFT Size (N_{fft})	128
Channel Taps (N_{taps})	128
No. of Symbols in OFDM Symbol (N_{sym})	128
Cyclic Prefix length (CP)	32
SNR Range	1:24 dB
Channel Realizations (N_{drops})	500
ISI Iterations (N_{isi})	6
PIC Stages (N_{pic})	4
Decision Device	Hard Decisions
ICI Scaling Factor	50 % 75 % 100 % 150 %

Table 6.3: Parameters/Variables implemented in ICI Scaling Scenario

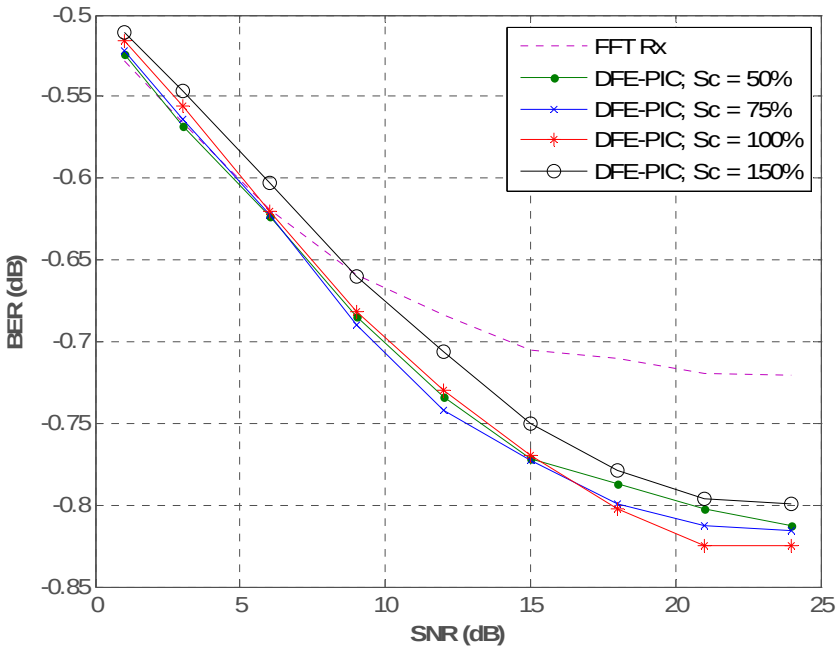

Figure 6.7: Performance Comparison of Effect of ICI Scaling

Figure 6.7 displays the performance of DFE-PIC receivers with different ICI scaling factors. We observe that as the scaling factor is decreased or increased away from 100%, there is performance degradation in the symbol estimation. The DFE-PIC receiver seems to work best at a scaling factor of 100%.

Although it should also be noted that at a scaling factor of 75%, the receiver works slightly better before an SNR of 15dB, than it does at 100% scaling. A likely reason for this trend may be that a slightly lesser scaling factor than 100% causes less ICI estimation errors to flow onto the next PIC stage. As such, it does show some amount of improvement, at least before 15dB SNR. However, the BER floor of 100% ICI scaled receiver is better than that of the 75% case.

Depending upon our system parameters and requirements, it may sometimes be beneficial to lower the ICI scaling factor, especially if the channel estimation is known to be somewhat inaccurate. However, generally the DFE-PIC receiver shows its best performance at a scaling factor of 100%.

6.4 SOFT DECISION SCALING FACTOR

PIC detector stages make use of decision devices in order to get better estimates of the symbols at each stage. This, in turn, helps form better ICI estimates in the next stage. Depending upon the type of PIC detector being implemented, a hard or a soft decision device may be utilized in each stage. Some PIC detectors make use of both kinds of decision devices at specific stages of the detector to get the best performance at the output.

In this scenario a PIC detector is implemented with only soft decisions being made at each stage. Such a PIC detector is termed as a linear PIC detector. The scaling factor of a soft-decision device represents the magnitude to which the decision will match an actual symbol value. Based on the detector's confidence of the estimated symbol, the scaling factor will shift the received values towards the actual values proportionally. The greater the value of the scaling factor, the more closely does the decision match that of a hard decision device.

If the detector is less confident about a symbol estimate, the soft decision device will not shift the estimated symbol close to its actual value. On the other hand, a hard decision device does not consider any confidence level on its decisions but converts all estimation to the actual amplitude values. This means that using a soft decision device lowers the errors that propagate to the next PIC stage as compared to the use of a hard decision device. Thus the soft decision based PIC performs better than the hard decision PIC detector.

The current scenario deals with the reaction of the DFE-PIC receiver to a variation of the soft decision scaling factor. Four different cases are implemented with a varying degree of soft scaling factor. The results of these simulations are shown in figure 6.8 where an improvement in BER is analyzed against an increase in SNR for each of the cases. Table 6.4 shows the parameters and variables used in the simulation of these cases.

FFT Size (N_{fft})	128
Channel Taps (N_{taps})	128
No. of Symbols in OFDM Symbol (N_{sym})	128
Cyclic Prefix length (CP)	32
SNR Range	1:24 dB
Channel Realizations (N_{drops})	500
ISI Iterations (N_{isi})	3
PIC Stages (N_{pic})	6
Decision Device	Soft Decisions
ICI Scaling Factor	100 %
Soft Decision Scaling Factor	50 % 100 % 200 % 400 %

Table 6.4: Parameters/Variables implemented in Soft Decision Scaling Scenario

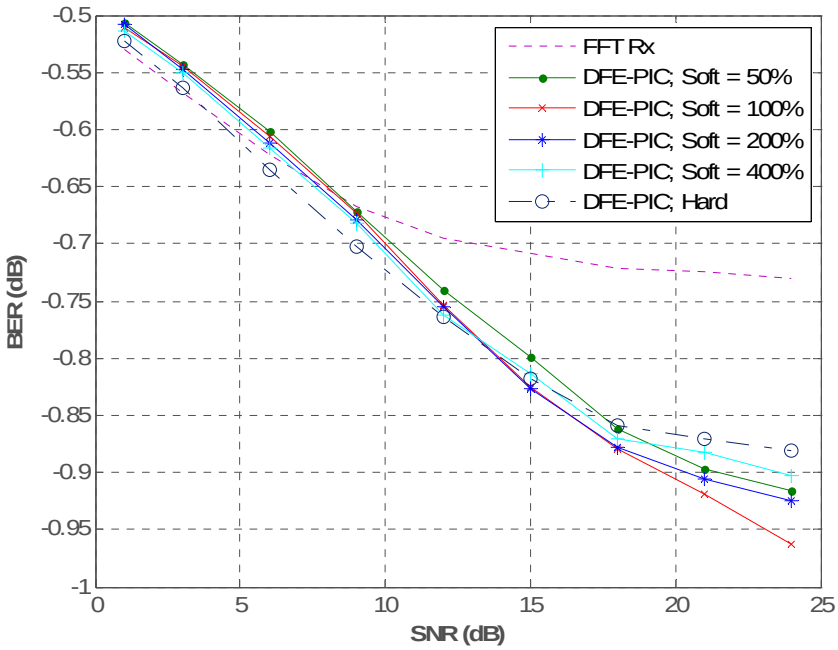

Figure 6.8: Performance Comparison of Effect of Soft Decision Scaling

Figure 6.8 displays that as the soft decision scaling factor is increased above 100%, the BER performance degrades more and more. Furthermore, as the scaling factor is increased, the performance starts to resemble that of a hard decision PIC detector. The reason for this is that with greater scaling factor values, erroneous decisions flow on to the next stages with higher amplitudes than with lesser scaling factor values. This causes more errors in the next stage's symbol estimates.

It is also observed that as the scaling factor is decreased below the value of 100%, the performance of the soft decision PIC suffers. A likely reason for this trend is the fact that scaling factors much lower than 100% do not allow the confident decisions to closely resemble actual decision amplitudes. This means that confident decisions do not end up matching actual decisions and this causes BER performance degradation. It is obvious that if a scaling factor much lesser than 100% is to be used, then we need to increase the number of PIC stages in order to get the same level of performance.

The results clearly display that a DFE-PIC receiver works best with soft decisions and a scaling factor of 100%. If the scaling factor is increased or decreased, then the performance of the receiver suffers. At the final SNR of 24 dB, the DFE-PIC receiver with 100% scaling factor shows a BER performance gain of approximately 0.25 dB in comparison with a conventional receiver.

6.5 CHOICE OF DECISION DEVICE

The type of decision-making device used in the receiver has a direct influence on the performance of the receiver. This thesis implements both hard and soft decision devices with varying configurations.

A hard decision device would allocate the actual symbol values to the estimated symbol whereas a soft decision device would drive closer to or away from the actual symbol values based on the confidence level of the decision. This means that an error in symbol estimation with a hard decision device would double in the next PIC stage, while with a soft decision device the effect on the next stage will be limited. This allows a soft decision-based PIC to perform better than a hard decision PIC detector.

The current scenario deals with the effect of different configurations of decision devices on the DFE-PIC receiver. Four different cases are implemented with different configurations. The results of these simulations are shown in figure 6.9 where an improvement in BER is analyzed against an increase in SNR for each of the cases. Table 6.5 shows the parameters and variables used in the simulation of these cases.

FFT Size (N_{fft})	128
Channel Taps (N_{taps})	128
No. of Symbols in OFDM Symbol (N_{sym})	128
Cyclic Prefix length (CP)	32
SNR Range	1:24 dB
Channel Realizations (N_{drops})	500
ISI Iterations (N_{isi})	3
PIC Stages (N_{pic})	6
Decision Device	Hard Decisions Soft Decisions
ICI Scaling Factor	100 %
Soft Decision Scaling Factor	100 %

Table 6.5: Parameters/Variables implemented in Decision Device Scenario

Apart from the implementation of a pure soft decision and a pure hard decision PIC detector, this scenario introduces two other PIC decision configurations:

- The first configuration utilizes soft decisions in all stages of the PIC detector with a hard decision being taken at the final output of the PIC detector. This configuration makes sure that before going through the feed-back loop, the symbol amplitudes match actual decision values allowing for a better estimation of ISI to be removed from the next incoming signal at the receiver.
- The second configuration utilizes soft decisions in stage 0 of the PIC detector with all other stages implementing hard decisions only. This configuration realizes the fact that stage 0 does not remove any ICI from the received signal and poses the greatest chance of producing errors. Hence using soft decisions at this stage will allow lesser errors to propagate to the next stages.

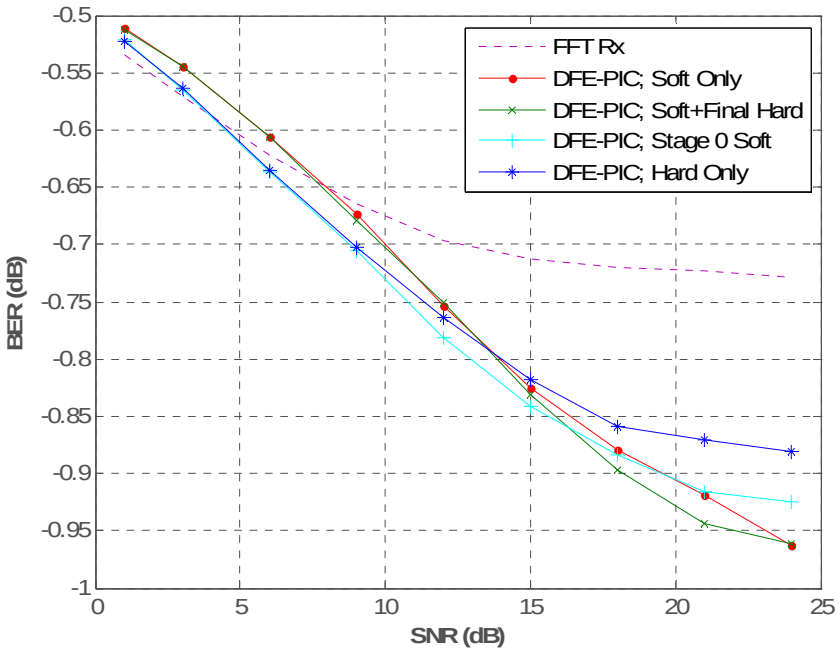

Figure 6.9: Performance Comparison of Effect of Decision Device

Figure 6.9 shows that the best BER performance is achieved by the configuration utilizing soft decisions in all PIC stages with a final hard decision before the feed-back loop. The soft decisions allow lesser errors to be generated while the final hard decision allows better ISI estimates to be cancelled out from the next symbol of the DFE. Utilizing pure soft decisions in the PIC detector seems to be the next best

receiver configuration. The soft decisions allow lesser errors to be transmitted along the PIC stages and the performance is excellent in this case.

The DFE-PIC receiver performs worst in the case of only hard-decisions being utilized in the PIC stages. This is clearly because of the doubling of errors from stage to stage, that is an inherent property of hard decision PIC detectors. The same reasoning is true for the receiver configuration where hard decisions are taken along all stages of PIC, except stage 0 which uses soft decisions only. In this configuration, the BER performance improves much more than the pure hard decision PIC detector. This provides good evidence that decreasing errors in stage 0 alone allows for far better performance due to less errors being propagated through the PIC stages.

It is worth observing that the worst two configurations mentioned above seem to out-perform the others until 15dB SNR, after which their performance deteriorates and a BER floor is reached. A likely reason for this trend is the fact that lower SNR values have stronger noise components to which the lesser confidence soft decisions are more sensitive. The stronger noise components may easily overcome the lesser confident decisions and cause random decisions that degrade performance within this SNR interval.

It is also interesting to note in figure 6.9, that the BER performance curve of pure soft decision receiver configuration does not floor out while the rest of the configurations do reach a floor level. It is quite possible that the soft decision configuration would outperform all other configurations at greater SNR values than the ones recorded here.

6.6 NUMBER OF CHANNEL TAPS

In OFDM-based systems, if the length of the channel's delay spread is less than the length of the cyclic prefix (CP), the CP absorbs the signal-deteriorating effects of the channel. This results in an ISI and ICI free reception of the transmitted signal. However, if the delay spread of the channel increases more than the length of the CP, ISI and ICI components contaminate the received signal and deteriorate the performance of the system. In order to improve the performance of the system in such conditions, a DFE-PIC detector has been implemented in the receiver.

This thesis simulates conditions where the delay spread of the channel is much greater than the length of the CP. The length of the delay spread of a channel is depicted by the number of taps of the channel that the receiver observes. In the current scenario, we deal with channels with varying number of channel taps and observe how the receiver behaves in varying channel conditions.

The current scenario deals with the reaction of the receiver to a variation in the number of channel taps. Four different cases are implemented with different channel situations. The results of these simulations are shown in figures 6.10 and 6.11 where an improvement in BER is analyzed against an increase in SNR for each of the cases. Table 6.6 shows the parameters and variables used in the simulation of these cases.

FFT Size (N_{fft})	128
Channel Taps (N_{taps})	128 96 64 32
No. of Symbols in OFDM Symbol (N_{sym})	128
Cyclic Prefix length (CP)	32
SNR Range	1:24 dB
Channel Realizations (N_{drops})	500
ISI Iterations (N_{isi})	6
PIC Stages (N_{pic})	4
Decision Device	Hard Decisions
ICI Scaling Factor	100 %

Table 6.6: Parameters/Variables implemented in Channel Taps Scenario

It is observed that as the length of the channel is increased, the performance of the conventional receiver deteriorates. With the implementation of the DFE-PIC receiver, a marked improvement in the performance occurs. However, the improvement that the receiver can achieve is still affected by the number of channel taps.

With lesser channel taps, the receiver is able to show huge improvements over a conventional receiver. With extreme cases where the channel taps are too great, the improvement, while still much better than the conventional receiver, starts relatively decreasing.

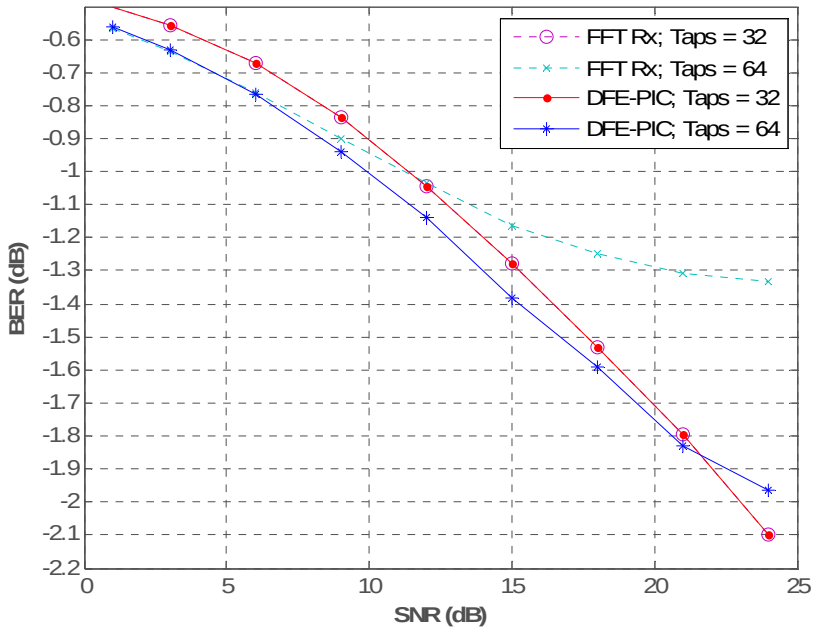

Figure 6.10: Performance Comparison with 32 and 64 Channel Taps

Figure 6.10 compares the performance of the conventional OFDM receiver to the DFE-PIC receiver in the cases of 32 and 64 channel taps. In the case of 32 taps, the same channel length as the length of the CP, we observe that the conventional OFDM receiver is able to cope with all interference present in the received signal. Since the DFE-PIC receiver has no interference to remove, there is no improvement in this case.

However, when the channel taps are doubled to 64, the conventional receiver's BER performance deteriorates by almost 0.8 dB while the DFE-PIC receiver is able to maintain its BER within 0.15 dB of the optimum zero-interference case with channel taps equal to the CP. In fact until approximately 21dB SNR, the DFE-PIC receiver maintains a better BER performance than with the zero-interference case. This goes on to show that apart from removing the interference, the DFE-PIC is able to cope with a certain level of noise components also.

Figure 6.11 compares the performance of the conventional OFDM receiver to the DFE-PIC receiver in the cases of 96 and 128 channel taps. It is observed that the DFE-PIC receiver provides a BER performance improvement of approximately 0.1 dB and 0.3 dB respectively in the case of 128 and 96 channel taps.

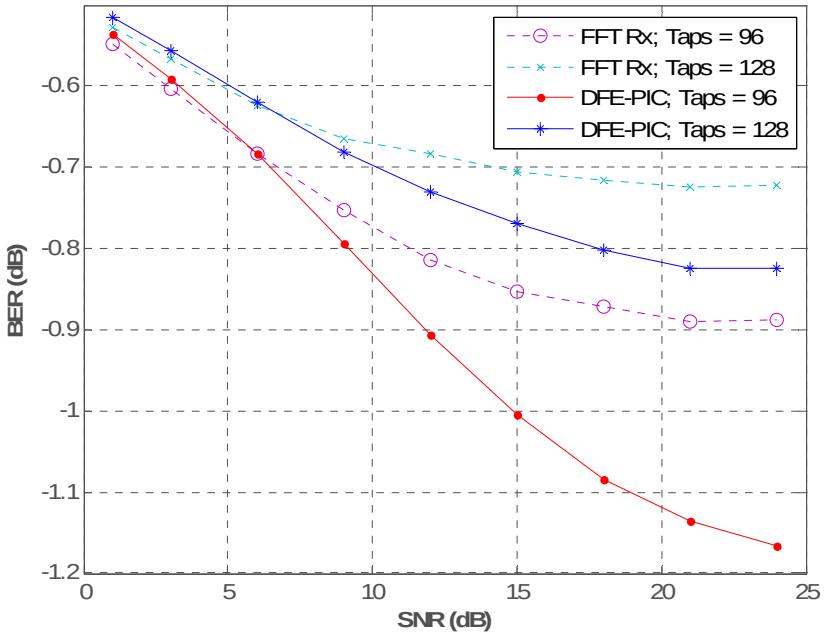

Figure 6.11: Performance Comparison with 96 and 128 Channel Taps

It is apparent from the figures that as the number of channel taps decrease, the ability of the proposed receiver to improve performance increases in comparison to the conventional receiver. Figure 6.11 shows a channel with an extreme delay spread condition where the number of channel taps is equivalent to the length of the transmitted symbol. However, even in such restrictive conditions the proposed receiver shows an improvement of 0.1 dB over the conventional receiver.

6.7 IMPLEMENTATION IN SIMULATED SFN CHANNELS

The previous sections dealt with the performance response of the proposed receiver to parameter variation in the worst-case channels. The channels implemented had delay spreads as long as the length of the transmitted OFDM symbol. The current scenario deals with the simulation of the proposed receiver in simulated SFN channels. These channels have been imported from the simulation work of [32].

The scenario deals with SFN channels from three cases where the inter-site distance (ISD) between the transmitters is varied and the performance of the proposed receiver is observed in such conditions. Furthermore, the channels used are of the worst-case users from each of these cases. These worst-case user channels are taken from the SINR CDF of the respective SFN at values of 0.5 %, 1.0% and 1.5% of the distribution. The performance of the proposed receiver is compared in each of these cases. Table 6.7 displays the parameters and the variables used in the scenario.

FFT Size (N_{fft})	128
Channel Taps (N_{taps})	128
No. of Symbols in OFDM Symbol (N_{sym})	128
Symbol Duration	102.4 μs
Cyclic Prefix length (CP)	32
CP Duration	26 μs
Inter-Site Distance (ISD)	5 Km 10 Km 20 Km
SNR Range	15:39 dB (5 Km) 9:34 dB (10 Km) 1:24 dB (20 Km)
Channel Realizations (N_{drops})	500
ISI Iterations (N_{isi})	4
PIC Stages (N_{pic})	4
Decision Device	Hard Decisions
ICI Scaling Factor	100 %

Table 6.7: Parameters/Variables implemented in SFN Scenario

6.7.1 PERFORMANCE ANALYSIS AT 5 KM ISD

This case simulates over SFN channels with an ISD of 5 Km. The proposed receiver is implemented over channels of different worst-case users taken from the SFN simulation. The distribution of SNR in correspondence with the CDF values at which these channels have been taken is shown in figure 6.12.

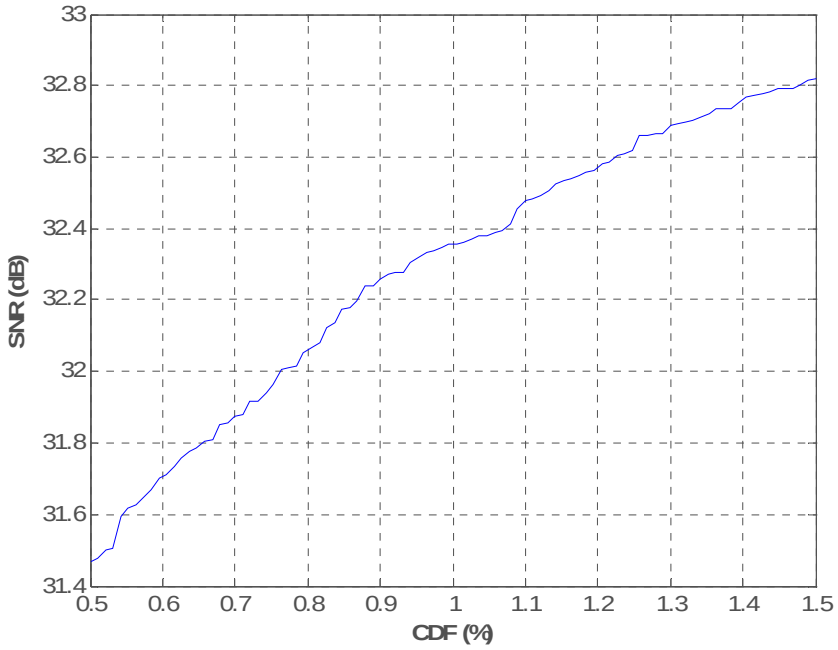

Figure 6.12: Distribution of channel SNR for SFN at 5 Km ISD

The SNR range over which this scenario is implemented has been maintained in accordance with the SNR range over which the channels have been taken from the SFN. These are observed in the SNR distribution of figure 6.12. The results of the simulations are shown in figures 6.13 to 6.15 where an improvement in BER is analyzed against an increase in SNR for each of the worst-case user channels.

The results in figures 6.13 to 6.15 show great improvement in the performance curves. It should be kept in mind that-these simulations have been executed over the worst-case users in the SFN and such performance improvement is of great value especially in such conditions.

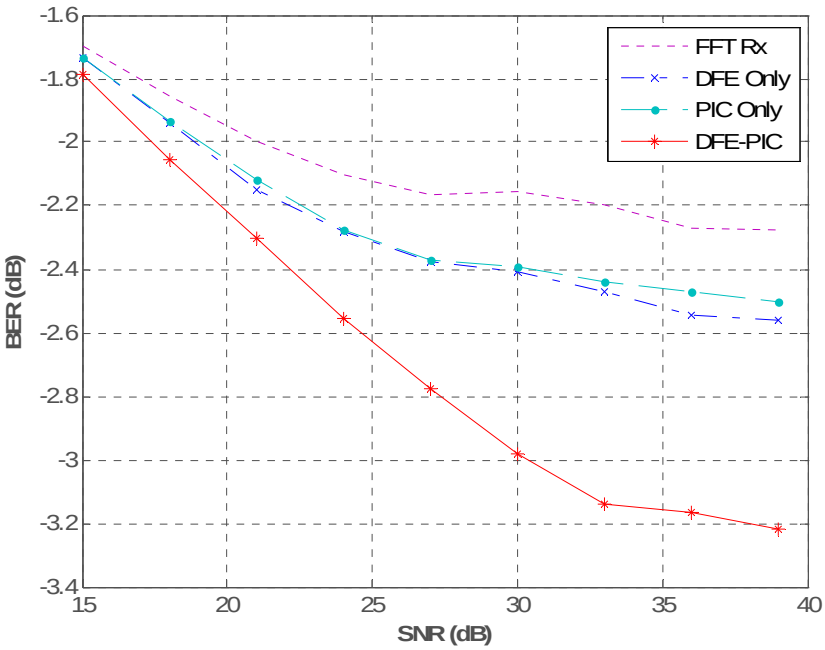

Figure 6.13: Performance of SFN at 5 Km ISD (0.5% CDF)

Figure 6.13 shows the simulation of a SFN channel at 0.5 % CDF. The SNR corresponding to 0.5 % CDF in figure 6.12 is 31.5 dB approximately. Figure 6.13 shows a clear BER performance improvement of almost 0.8 dB at an SNR of 31 dB.

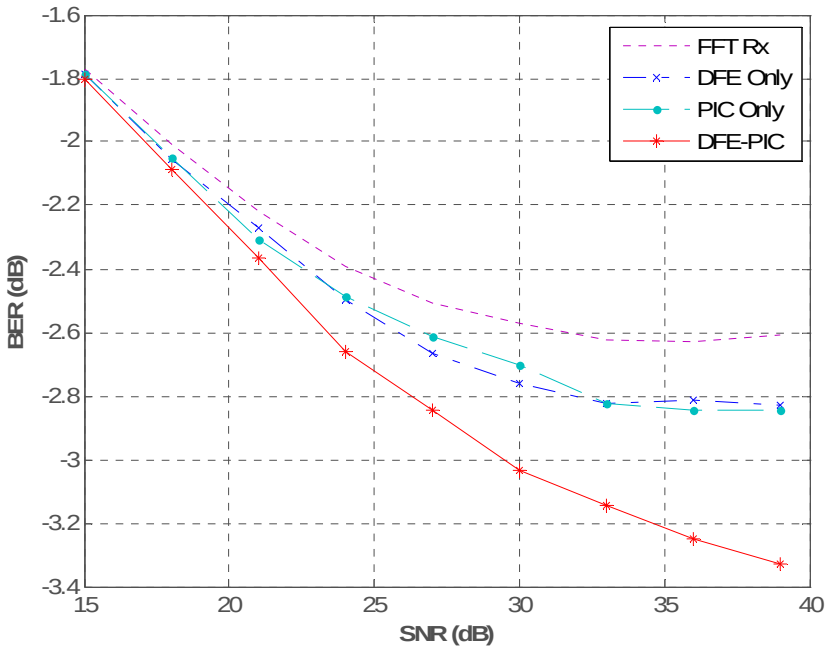

Figure 6.14: Performance of SFN at 5 Km ISD (1.0% CDF)

Figure 6.14 shows the simulation of a SFN channel at 1.0 % CDF. The SNR corresponding to 1.0 % CDF in figure 6.12 is 32.4 dB approximately. Figure 6.14 shows a clear BER performance improvement of almost 0.5 dB at an SNR of 32.5 dB.

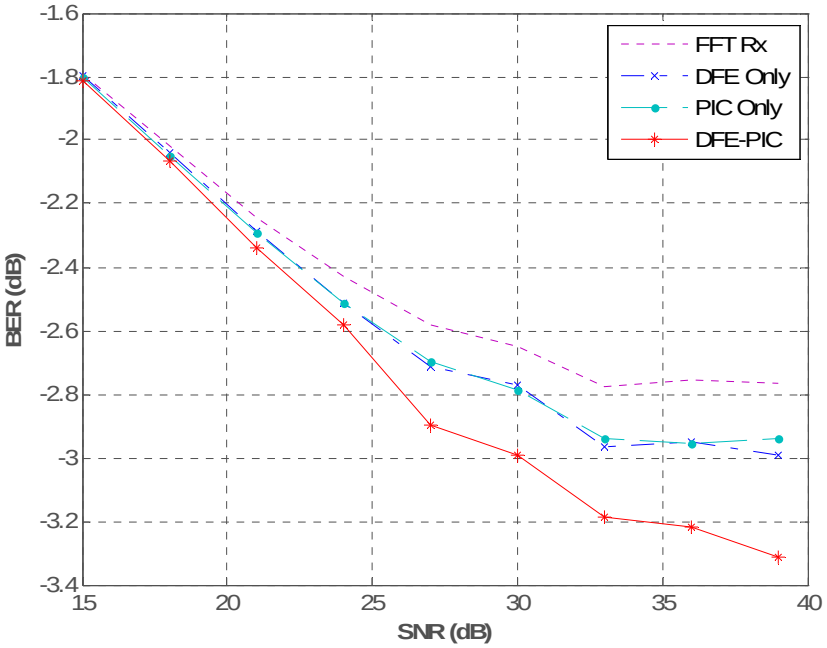

Figure 6.15: Performance of SFN at 5 Km ISD (1.5% CDF)

Figure 6.15 shows the simulation of a SFN channel at 1.5 % CDF. The SNR corresponding to 1.5 % CDF in figure 6.12 is 32.8 dB approximately. Figure 6.15 shows a clear BER performance improvement of almost 0.4 dB at an SNR of 32.8 dB.

A point well-worth mentioning in these results is the performance improvement of the PIC-only symbol estimations. In all of the cases, the PIC-only curve improves well over the channel estimation curve of the received signal and closely matches the performance improvement achieved by the process of ISI-removal.

6.7.2 PERFORMANCE ANALYSIS AT 10 KM ISD

This case simulates over SFN channels with an ISD of 10 Km. The proposed receiver is implemented over channels of different worst-case users taken from the SFN simulation. The distribution of SNR in correspondence with the CDF values at which these channels have been taken is shown in figure 6.16.

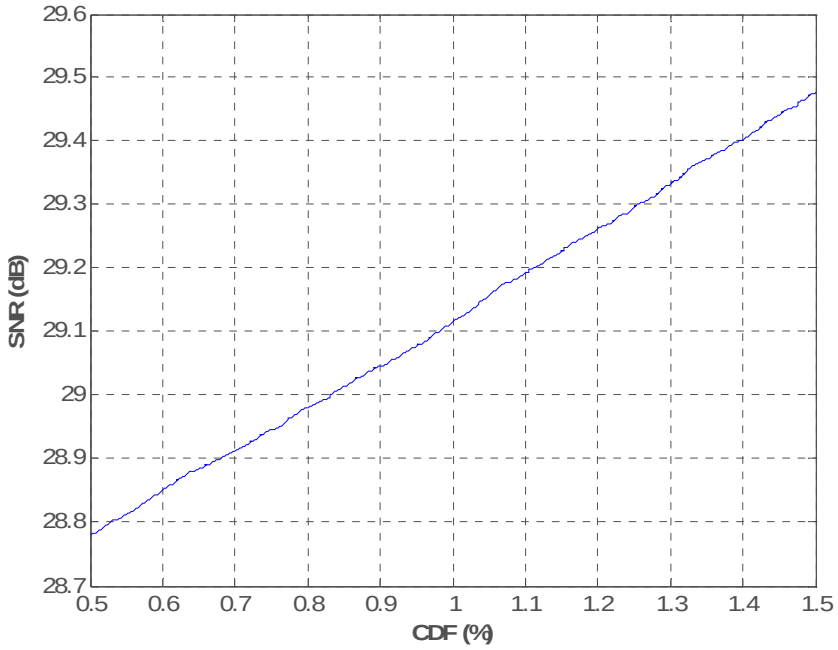

Figure 6.16: Distribution of channel SNR for SFN at 10 Km ISD

The SNR range over which this scenario is implemented has been maintained in accordance with the SNR range over which the channels have been taken from the SFN. These are observed in the SNR distribution of figure 6.16. The results of the simulations are shown in figures 6.17 to 6.19 where an improvement in BER is analyzed against an increase in SNR for each of the worst-case user channels.

The results in figures 6.17 to 6.19 show great improvement in the performance curves. It should be kept in mind that-these simulations have been executed over the worst-case users in the SFN and such performance improvement is of great value especially in such conditions.

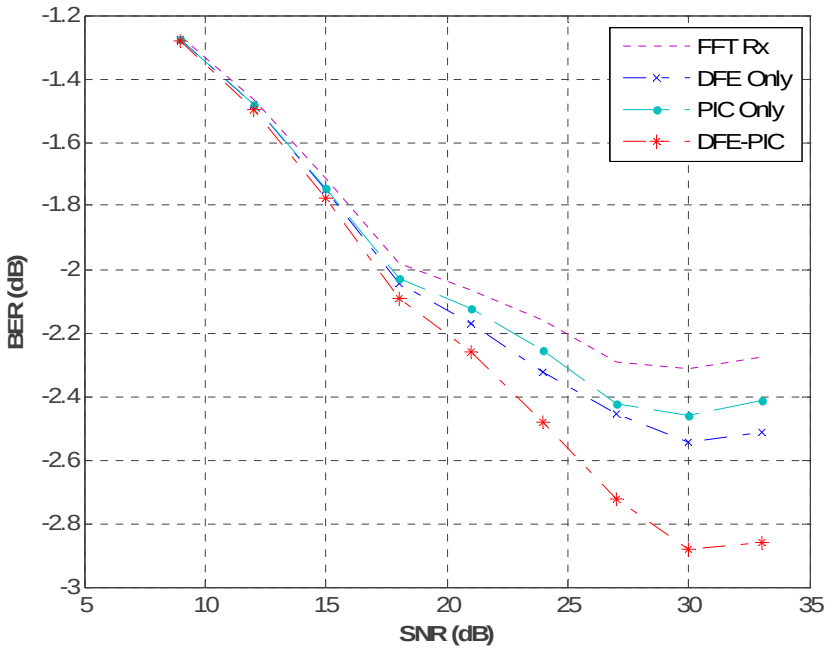

Figure 6.17: Performance of SFN at 10 Km ISD (0.5% CDF)

Figure 6.17 shows the simulation of a SFN channel at 0.5 % CDF. The SNR corresponding to 0.5 % CDF in figure 6.16 is 28.8 dB approximately. Figure 6.17 shows a clear BER performance improvement of almost 0.6 dB at an SNR of 29 dB.

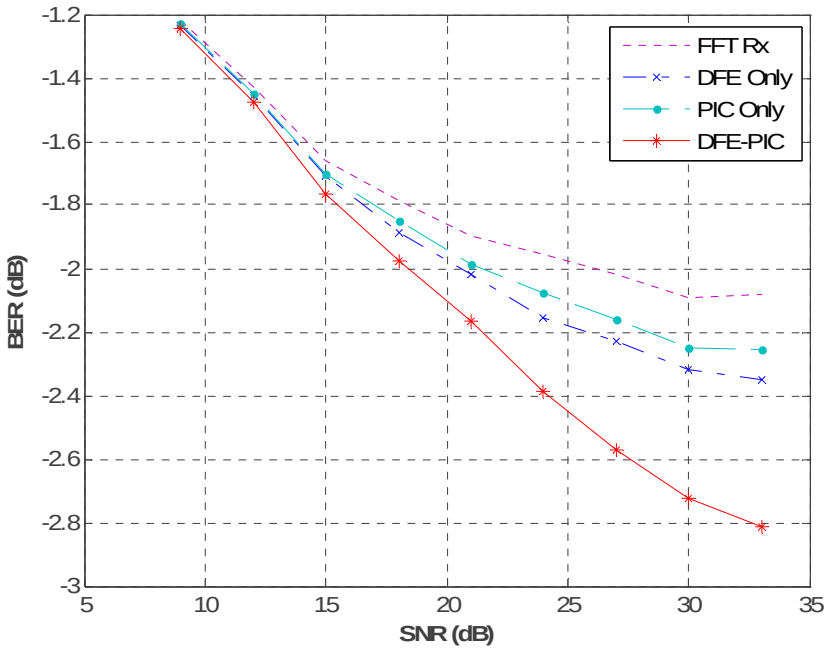

Figure 6.18: Performance of SFN at 10 Km ISD (1.0% CDF)

Figure 6.18 shows the simulation of a SFN channel at 1.0 % CDF. The SNR corresponding to 1.0 % CDF in figure 6.16 is 29.1 dB approximately. Figure 6.18 shows a clear BER performance improvement of almost 0.6 dB at an SNR of 29 dB.

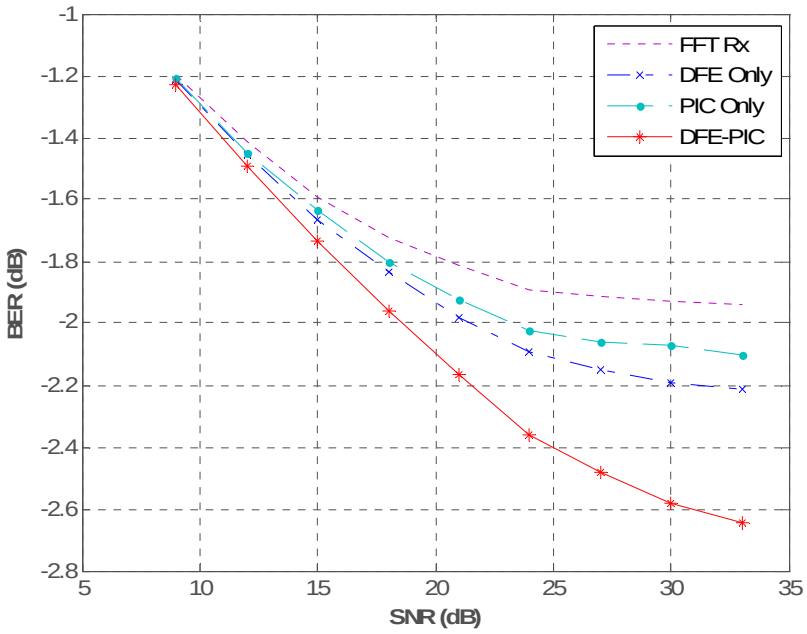

Figure 6.19: Performance of SFN at 10 Km ISD (1.5% CDF)

Figure 6.19 shows the simulation of a SFN channel at 1.5 % CDF. The SNR corresponding to 1.5 % CDF in figure 6.16 is 29.5 dB approximately. Figure 6.19 shows a clear BER performance improvement of almost 0.65 dB at an SNR of 29.5 dB.

As observed in the previous case, the PIC-only curve improves well over the channel estimation curve of the received signal and closely matches the performance improvement achieved by the process of ISI-removal.

6.7.3 PERFORMANCE ANALYSIS AT 20 KM ISD

This case simulates over SFN channels with an ISD of 20 Km. The proposed receiver is implemented over channels of different worst-case users taken from the SFN simulation. The distribution of SNR in correspondence with the CDF values at which these channels have been taken is shown in figure 6.20.

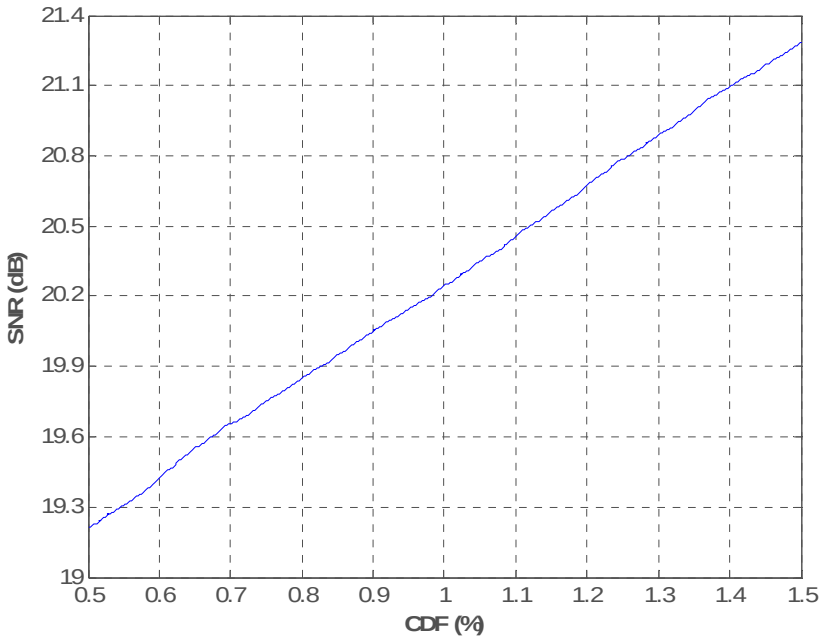

Figure 6.20: Distribution of channel SNR for SFN at 20 Km ISD

The SNR range over which this scenario is implemented has been maintained in accordance with the SNR range over which the channels have been taken from the SFN. These are observed in the SNR distribution of figure 6.20. The results of the simulations are shown in figures 6.21 to 6.23 where an improvement in BER is analyzed against an increase in SNR for each of the worst-case user channels.

The results in figures 6.21 to 6.23 show great improvement in the performance curves. It should be kept in mind that-these simulations have been executed over the worst-case users in the SFN and such performance improvement is of great value especially in such conditions.

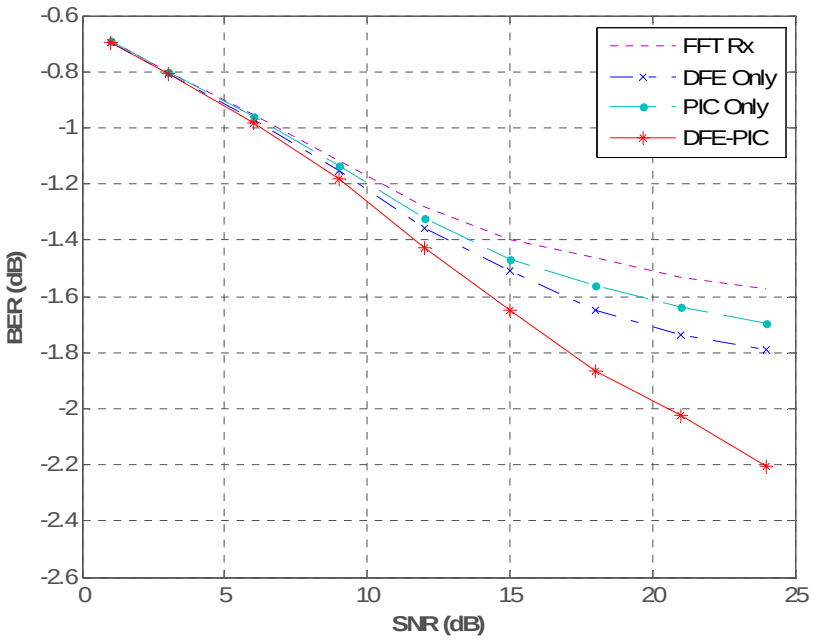

Figure 6.21: Performance of SFN at 20 Km ISD (0.5% CDF)

Figure 6.21 shows the simulation of a SFN channel at 0.5 % CDF. The SNR corresponding to 0.5 % CDF in figure 6.20 is 19.2 dB approximately. Figure 6.21 shows a clear BER performance improvement of almost 0.5 dB at an SNR of 19 dB.

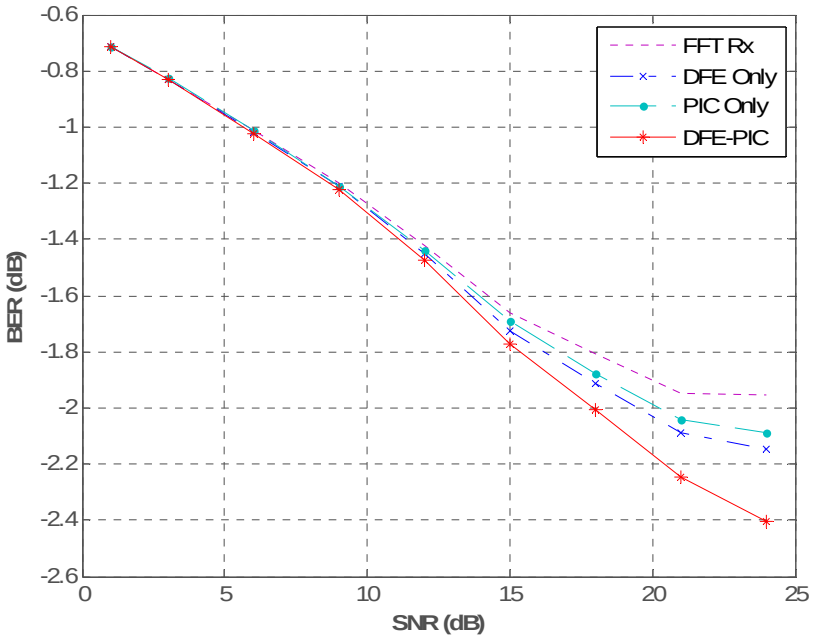

Figure 6.22: Performance of SFN at 20 Km ISD (1.0% CDF)

Figure 6.22 shows the simulation of a SFN channel at 1.0 % CDF. The SNR corresponding to 1.0 % CDF in figure 6.20 is 20.2 dB approximately. Figure 6.22 shows a clear BER performance improvement of almost 0.3 dB at an SNR of 20 dB.

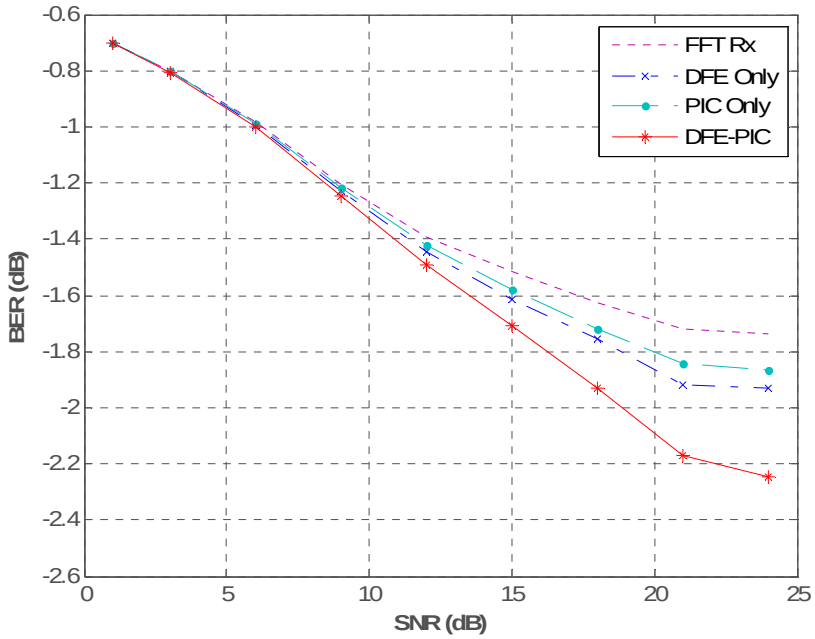

Figure 6.23: Performance of SFN at 20 Km ISD (1.5% CDF)

Figure 6.23 shows the simulation of a SFN channel at 1.5 % CDF. The SNR corresponding to 1.5 % CDF in figure 6.20 is 21.3 dB approximately. Figure 6.23 shows a clear BER performance improvement of almost 0.4 dB at an SNR of 21 dB.

As observed in the previous cases, the PIC-only curve improves well over the channel estimation curve of the received signal and closely matches the performance improvement achieved by the process of ISI-removal.

It is quite clear from these results that the proposed receiver offers huge benefits over the conventional receiver especially in SFN environments. Maintaining such level of performance improvement in channels with long delay spreads is especially beneficial for the worst case users as has been shown in the results.

CHAPTER 7

CONCLUSIONS

7.1 Conclusions

This thesis proposes an improved receiver design for channels with long delay spreads. These types of channels are present in Single Frequency Networks (SFN) used for DVB-T broadcast systems. The proposed receiver implements a Parallel Interference Canceller (PIC) detector within a Decision Feedback Equalizer (DFE) configuration.

The performance of the proposed receiver is compared with the performance of the conventional receiver in such SFN channels. The performance is analyzed in terms of an improvement in BER with respect to a variation in SNR. Various parameters of the receiver design are investigated and their effect on the BER performance is analyzed. Performance is further investigated over simulated SFN channels and the worst-case scenarios of such channels.

Considering the variation in the number of ISI iterations it is observed that as the ISI iterations increase, the BER performance deteriorates. This is because each iteration cancels ISI based on the previously-estimated symbol, and errors from previous iterations cause a growing trend of errors in later iterations. In practice, the problem of such error propagation is resolved by the periodic transmission of a training sequence which allows the receiver to synchronize its detector decisions.

On the other hand, an increase in the number of PIC stages improves the symbol estimation. This is because each additional stage provides a more accurate estimate of the ICI which allows better estimates of the symbols. Hence the BER performance

improves with an increase in the number of PIC stages. In the same context, the effect of variation in the ICI scaling factor is also investigated. It is shown that the best performance is achieved when 100% of the ICI is removed. However, in case of inaccurate channel estimation, a slight decrease in the ICI scaling factor might prove to be beneficial as it limits the error to grow uncontrollably.

Different configurations of hard and soft decision devices are implemented in the receiver and their performance analyzed. It is observed that the soft decision PIC with a final stage hard decision performs the best, due to its lower error propagation from stage to stage and its more accurate ISI cancellation properties. The hard decision PIC detector provides the worst performance due to its error doubling issue. Furthermore, variation in the scaling factor of the soft decisions shows that the receiver performs best with scaling factor closer to 100%.

The effect of variation of the channel delay spread is also investigated. It is observed that the performance of the receiver improves as the number of channel taps is decreased. As the number of channel taps decrease, the ability of the proposed receiver to estimate symbols gets better. This results in a greater performance improvement in comparison to the conventional receiver.

Finally, the proposed receiver is implemented in a simulated SFN environment. Worst-case user channels are picked and the performance improvement of the receiver is compared with that of the conventional receiver. It is observed that the proposed receiver greatly out-performs the conventional receiver in recovering from the mitigating effects of the SFN channels.

The proposed receiver design holds much promise for OFDM-based systems in SFN environments. Significant performance improvement was observed in the outcome of the simulation results. Furthermore, this gain is achieved without any extra signaling or significant increase in the complexity of the receiver.

REFERENCES

[1] D. Starobinski, "Users Mobility and Call Blocking in Wireless Networks." Available online 17th of May 2008 at: http://people.bu.edu/staro/img1.gif

[2] C. Langton, "Orthogonal Frequency Division Multiplex (OFDM) Tutorial." Available online 17th of May 2008 at: http://www.complextoreal.com/chapters/ofdm2.pdf

[3] "Digital Video Broadcasting Project (DVB)." Available online 17th of May 2008 at: http://www.dvb.org/

[4] M. A. Hasan, "Performance Evaluation of WiMAX/IEEE 802.16 OFDM Physical Layer," M.Sc. Thesis report, Helsinki University of Technology (TKK), June 2007.

[5] WiMAX Forum, "White paper on Mobile WiMAX – Part 1: A Technical Overview and Performance Evaluation,"August 2006. Available online 17th of May 2008 at: http://www.wimaxforum.org/technology/downloads/Mobile_WiMAX_Part1_Overview_and_Performance.pdf

[6] M. Munster, "Wireless Multi-user OFDM Systems," Article available online 17th of May 2008 at: http://www-mobile.ecs.soton.ac.uk/comms/Res_Int_transceiver.htm

[7] J. H. Stott, "The how and why of COFDM," BBC Research and Development Tutorial, 1998. Available online 17th of May 2008 at: http://www.ebu.ch/en/technical/trev/trev_278-stott.pdf

[8] J. Cai, W. Song, Z. Li, "Doppler Spread Estimation for Mobile OFDM Systems in Rayleigh Fading Channels," IEEE Transactions on Consumer Electronics, Vol. 49, Issue 4, Nov. 2003, pp. 973-977.

[9] Tutorial on "COFDM", Digital Radio Technology. Available online 17th of May 2008 at: http://www.digitalradiotech.co.uk/cofdm.htm

[10] O. Miliet, "Technical Overview on Single Frequency Networks," White paper, EnenSys Technologies. Available online 17th of May 2008 at: http://www.enensys.com/resources/support/White_papers/Single_frequency_network_overview_ENENSYS.pdf

[11] A. Ligeti, "Single Frequency Network Planning," PhD dissertation, Kungl Tekniska Högskolan, September 1999, ISRN-KTH/RST/R-99/11-SE. Also available online 17th of May 2008 at: http://www.diva-portal.org/diva/getDocument?urn_nbn_se_kth_diva-2857-2_fulltext.pdf

[12] H. Sari, G. Karam, I. Jeanclaude, "Transmission Techniques for Digital Terrestrial TV Broadcasting," IEEE Communications Magazine, 0163-6804/95/$04.00, February 1995.

[13] D. Lung, "Single Frequency Networks for DTV," TV Technology: RF Technology, article published in May 2003. Available online 17th of May 2008 at: http://www.tvtechnology.com/features/On-RF/f_dl_rf_technology.shtml

[14] T. Do-Hong, M. Selik, R. Baraniuk, M. Haag, C. S. Burrus, B. Aazhang, N. Kingsbury, H. Ta-Hong, T. Do-Ngoc, S. Nguyen-Le, "Principles of Digital Communications," Student Manual, Rice University. Available online 17th of May 2008 at: http://cnx.org/content/col10474/1.7/

[15] S. Benedetto, E. Biglieri, "Principles of Digital Transmission: With Wireless Applications," Published December 1998, Plenum Publishing Corporation, ISBN-13: 9780306457531.

[16] Y. Sun, "Bandwidth-efficient Wireless OFDM," IEEE Journal on Selected Areas in Communications, Vol. 19, Issue 11, November 2001, pp. 2267-2278.

[17] T. Laakso, “Signal Processing in Telecommunications I,” Lecture Notes (S-88.2211), Department of Electrical and Communications Engineering, Helsinki University of Technology (TKK), March 2006.

[18] Z. Tian, “Mitigating Error Propagation in Decision-Feedback Equalization for Multiuser CDMA,” IEEE Transactions on Communications, Vol. 52, Issue 4, April 2004, pp. 525-529.

[19] P. Ang, “Multiuser Detection for CDMA Systems,” Lecture Presentation, April 2001. Available online 17th of May 2008 at: http://wsl.stanford.edu/~ee360/mud_peter.ppt

[20] R. Lakshmish, “Hard Decision Parallel Interference Cancellation for Uplink OFDMA,” In the Joint International Conference on Optical Internet and Next Generation Network, July 2006, pp. 241-244, Digital Object Identifier: 10.1109/COINNGNCON.2006.4454681.

[21] J. G. Proakis, “Digital Communications,” 2nd Edition, McGraw Hill, 1989, ISBN-13: 978-0070517264.

[22] A. Duel-Hallen, J. Holtzman, Z. Zvonar, “Multiuser Detection for CDMA Systems,” IEEE Journal on Personal Communications, Vol. 2, Issue 2, April 1995, pp. 46-58.

[23] S. Moshavi, “Multi-user Detection for DS-CDMA Communications,” IEEE Communications Magazine, Vol. 34, Issue 10, October 1996, pp. 124-136.

[24] S. Verdu, “Multiuser Detection,” Cambridge University Press, August 1998, ISBN-13: 978-0521593731.

[25] S. Moshavi, “Survey of Multi-user Detection for DS-CDMA Systems,” Bellcore Publishers, IM-555, August 1996.

[26] S. Moshavi, E. G. Kanterakis, D. L. Schilling, ”Multistage Linear Receivers for DS-CDMA Systems,” International Journal of Wireless Information Networks, Vol. 3, No. 1, January 1996.

[27] V. Tikiya, A. Chockalingam, “A Threshold-based Linear Parallel Interference Canceller on Fading Channels,” In the 2005 IEEE Wireless Communications and Networking Conference, Vol. 2, March 2005, pp. 917-921.

[28] D. R. Brown III, M. Motani, V. V. Veeravalli, H. V. Poor, C. R. Johnson Jr., “On the Performance of Linear Parallel Interference Cancellation,” IEEE Transactions on Information Theory, Vol. 47, Issue 5, July 2001, pp. 1957-1970.

[29] D. Guo, L. K. Rasmussen, T. J. Lim, ”Linear Parallel Interference Cancellation in long-code CDMA multi-user detection,” IEEE Journal on Selected Areas in Communications, Vol. 17, Issue 12, December 1999, pp. 2074-2081.

[30] D. Divsalar, M. K. Simon, D. Raphaeli, “Improved Parallel Interference Canellation for CDMA,” IEEE Transactions on Communications, Vol. 46, Issue 2, February 1998, pp. 258-268.

[31] P. Patel, J. Holtzman, “Performance comparison of a DS/CDMA System using a Successive Interference Cancellation (IC) scheme and a Parallel IC scheme under Fading,” Proceedings International Conference on Communications, May 1994, Vol.1, pp. 510-514.

[32] Z. A. Qureshi, “Simulation of Single Frequency Network for Terrestrial Digital Video Broadcasting,” Special Assignment, Department of Electrical and Communications Engineering, Helsinki University of Technology (TKK), November 2007.

[33] F. Eory, “Comparison of Adaptive Equalization methods for the ATSC and DVB-T Digital Television Broadcast Systems,” Proceedings of the 2000 Third IEEE International Caracas Conference on Devices, Circuits and Systems, March 2000, pp. T107/1- T107/7.

[34] H. Yu, M. S. Kim, T. Jeori, S. K. Lee, ”Equalization scheme for OFDM Systems in long Delay Spread Channels,” 15th IEEE International Symposium on Personal, Indoor and Mobile Radio Communications, PIMRC, Vol. 2, September 2004, pp. 1297-1301.

[35] H. Wang, Z. Li, J. Lilleberg, “Equalizaed Parallel Interference Cancellation for MC-CDMA multi-code downlink transmissions,” IEEE Wireless Communications and Networking Conference, Vol. 3, March 2004, pp. 1812-1816.

[36] Resource on “Discrete Fourier Transform,” Wolfram MathWorld. Available online 17th May 2008 at: http://mathworld.wolfram.com/DiscreteFourierTransform.html

APPENDIX-A

CHANNEL SENSIBILITY TEST

A sensibility test was carried out to confirm whether the simulator channel matched with actual transmission channels. For this purpose, the number of channel taps was decreased to the CP length and the simulator was executed. The resulting BER curve from the simulator matched exactly with the BER curve of a normal QPSK Rayleigh channel. This step verified that our channel model was implemented correctly. The following figure displays the simulator calibration test result, which is exactly the same as the literature curve.

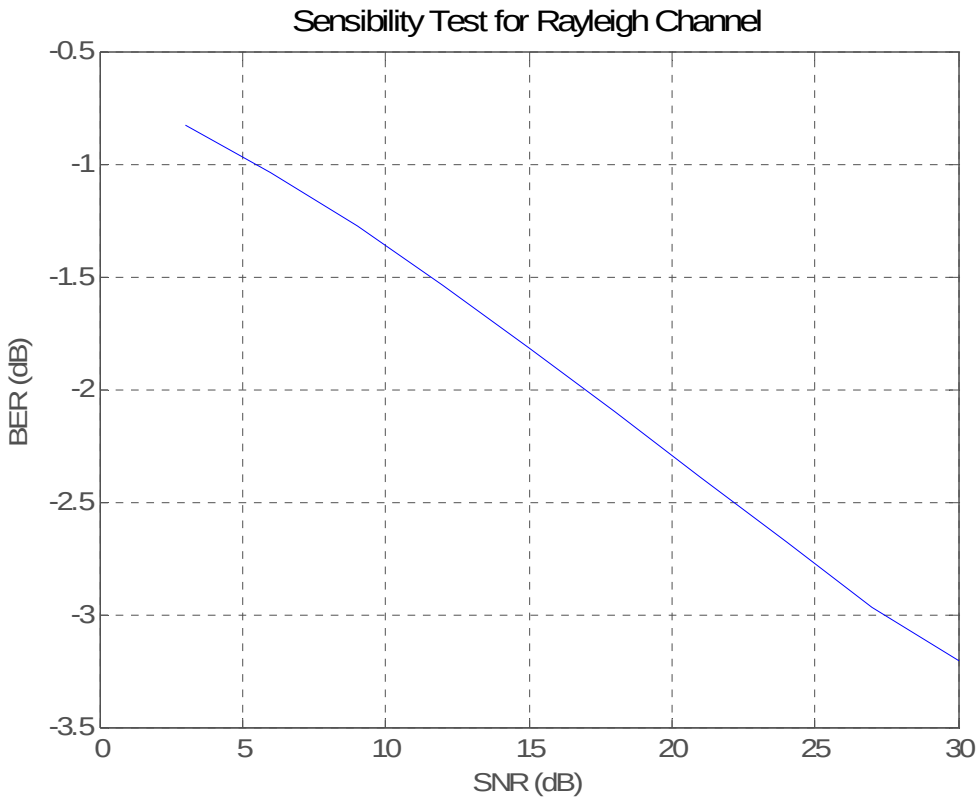

APPENDIX-B

MATLAB SIMULATION CODE

The MATLAB simulation code for the basic configuration of the receiver is detailed below. Each function is detailed under a separate heading.

MAIN FUNCTION OF THE CODE

```
clear all;
close all;
clc;

%%%%% System Parameters
%% FFT size
Nfft = 128;
%% Number of QPSK Symbols used
QPSK = 4;
%% Total number of Symbols in OFDM Symbol
Nsym = Nfft;
CP = ceil(Nfft/4);
%% Number of SNR loops
Nsnr = 9;
%% Number of Channel Realization loops
Ndrops = 5;
%% Number of ISI iterations
Nisi = 6;
%% Number of PIC Stages (excluding Stage 0)
Nici = 4;


%%%%% Initialization of General Variables
SNR         = [];
BER_conv    = [];
BER_isi     = [];
BER_pic     = [];
BER_dfe     = [];

%%%%% Importing the SFN TDL
% PDP = sfnPDP(Nfft, ISD);
% PDP = fliplr(PDP);
% PDP = PDP/sum(PDP);
% Ntaps = length(PDP);
%% Generating a Dummy PDP for testing purpose
Ntaps   = Nfft;
PDP     = ceil(10*rand(1,Ntaps));
PDP     = PDP/sum(PDP);


%%%%% Generating QPSK Symbol Library (Gray Coded)
symlib      = exp(j*2*pi*(0:(QPSK-1))/QPSK + j*pi/QPSK);
```

```
temp        = symlib(4);
symlib(4)   = symlib(3);
symlib(3)   = symlib(2);
symlib(2)   = temp;


%%%%% Starting SNR loop
for snrloop = 1:Nsnr

    if (snrloop == 1)
        snr = 1;
    else
        snr = (snrloop-1)*3;
    end

    %% Calculating normalized Noise Component based on SNR
    noise_sigma = sqrt(1/Nfft)*10^(-snr/20);

        %%%% Starting Channel Realization loop
    for drops = 1:Ndrops

        %% Generating Normally-Distributed Random Channel Realizatons
        h = (randn(1,Ntaps) + i*randn(1,Ntaps))/sqrt(2);
        h = h.*sqrt(PDP);

        Xchannel    = zeros(2*(Nfft+CP),1);
        hchannel    = zeros(1,size(Xchannel,1));
        shift       = size(hchannel,2) - Nfft + 1;
        hchannel(:,(shift-Ntaps+1):shift) = h;

        %% Determining ISI components
        hISI = zeros(1,size(Xchannel,1));
        hISI(:,(shift-Ntaps+1):(shift-CP-1)) = h(:,1:(Ntaps-CP-1));

        for ii = 1:Nfft
            ISI(ii,:) = circshift(hISI, [0 (ii-1)]);
        end

        hISI = zeros(Nfft,size(Xchannel,1));
        hISI(:,1:(size(Xchannel,1))/2)
                       = ISI(:,1:(size(Xchannel,1))/2);

        %% Determining ICI components (Designed to handle
        %% Ntaps=Nfft+2*CP)
        ICI = zeros(Nfft);

        if (Ntaps>Nfft)
            h1  = zeros(1,Ntaps);
            h1(:,1:(Ntaps-Nfft)) = fliplr(h(:,1:(Ntaps-Nfft)));
            h0  = h(:,(Ntaps-Nfft+1):Ntaps);
            Nh0 = length(h0);

            for ii = Nfft:-1:(Nfft-CP+1)
                for jj = ii:Nfft
                    ICI(jj,ii) = h1(:,(jj-ii+1));
                end
            end
        else
            h0  = h;
            Nh0 = length(h0);
        end
```

```
        count = Nfft - Nh0;

        for ii = (count+2):(Nfft-CP)
            for jj = 1:(ii-count-1)
                ICI(jj,ii) = -h0(:,(ii-jj-count));
            end
        end

        hICI = zeros(Nfft,size(Xchannel,1));
        hICI(:,(size(Xchannel,1)-Nfft+1):size(Xchannel,1)) = ICI;

        %% Determining lambda: Diagonal Matrix composed of
        %% Channel taps
        if (Ntaps>Nfft)
            lambda = fliplr(h(:,(Ntaps-Nfft+1):Ntaps));
        else
            lambda = zeros(1,Nfft);
            lambda(:,1:Ntaps) = fliplr(h);
        end

        lambda = diag(fft(lambda));


        %%% Starting the ISI iterrations
        for isiloop = 1:Nisi

            %% Generation of Noise signal components
            noise = noise_sigma.*(randn(Nfft,1)
                                  + i*randn(Nfft,1))/sqrt(2);

            %% Replacing Previous Symbol (exXo=Estimated
            %% and exX=Actual)
            %% This step simulates the DFE feed-back
            if (isiloop == 1)
                exXo    = zeros(size(Xchannel,1)/2,1);
                exX     = exXo;
            else
                exXo    = zeros(size(Xchannel,1)/2,1);
                exXo((CP+1):length(exXo),:)
                        = ifft(Sym_dfe/norm(Sym_dfe))*sqrt(Nfft);
                exXo(1:CP,:) = exXo((Nfft+1):(Nfft+CP),:);
                exX     = X;
            end

            %% Generating Current Transmitted Symbol
            [X, S, binarymap] = SymGen(symlib, QPSK, Nsym, Nfft, CP);

            %% Xchannel are the actual transmitted symbols
            Xchannel    = [exX; X];
            %% Xochannel is the estimated symbol from DFE Feedback
            Xochannel   = [exXo; zeros(size(X,1),1)];

            %% Implementing Channel Convolution of Transmitted Signal
            %% based on Actual Symbols. Simulates Channel Effect
            for ii = 1:Nfft
                RxY(ii,:) = circshift(hchannel, [0 (ii-1)])*Xchannel;
            end

%             %% Confirming the accuracy of ISI/ICI components
%             Hchannel = zeros(Nfft,size(Xchannel,1));
```

```
%             Hchannel(:,(size(Xchannel,1)-Nfft+1):size(Xchannel,1))
                                = ifft(ifft(lambda)')'*Nfft;
%             %% If testY is equal to RxY, the ISI/ICI components are
%             %% accurate
%             testY = Hchannel*Xchannel + hICI*Xchannel +
                                hISI*Xchannel;
%             RxY - testY


            %% Adding Normally-Distributed random Noise components to
            %% Recieved Signal. Simulates Channel's Noise insertion
            RxY = RxY + noise;

            %% Estimation of Symbol directly based on the Received
            %% Signal at the Rx input. Represents Conventional Rx
            Sym_conv = inv(lambda)*fft(RxY);

            %% Removal of ISI components based on Previous Estimated
            %% Symbol
            Ynoisi      = RxY - hISI*Xochannel;
            %% Estimation of Symbol after ISI removal
            Sym_noisi   = inv(lambda)*fft(Ynoisi);


            %% Implementation of PIC Detector for PIC-Only
            %% and Post-DFE
            %% Symbol Estimation
            Ypic = RxY;
            Ydfe = Ynoisi;
            %% Selecting MAI and Soft-Decision Scaling Factor Values
            scale       = 1;
            softscale   = 1*(sqrt(2)*2);
            %% Deriving Initial Observations
            zpic(:,1)   = fft(Ypic);
            zdfe(:,1)   = fft(Ydfe);
            %% Stage 0 Symbol Estimation
            spic(:,1)   = inv(lambda)*zpic(:,1);
            sdfe(:,1)   = inv(lambda)*zdfe(:,1);

            %% Choose Decision Device Configuration for PIC
            % Soft Decisions
            spic(:,1)   = (tanh(real(spic(:,1))*softscale)
                  + i*tanh(imag(spic(:,1))*softscale))/sqrt(2);
            sdfe(:,1)   = (tanh(real(sdfe(:,1))*softscale)
                  + i*tanh(imag(sdfe(:,1))*softscale))/sqrt(2);
            % Hard Decisions
            spic(:,1)   = Harddecide(spic(:,1), symlib, Nsym);
            sdfe(:,1)   = Harddecide(sdfe(:,1), symlib, Nsym);

            %% Implementation of PIC Stages after Stage 0
            for ii = 2:(Nici+1)
                zpic(:,ii)  = zpic(:,1)
                  - scale*(fft(fft(ICI')')/Nfft)*spic(:,(ii-1));
                zdfe(:,ii)  = zdfe(:,1)
                  - scale*(fft(fft(ICI')')/Nfft)*sdfe(:,(ii-1));
                spic(:,ii)  = inv(lambda)*zpic(:,ii);
                sdfe(:,ii)  = inv(lambda)*zdfe(:,ii);
                spic(:,ii)  = (tanh(real(spic(:,ii))*softscale)
                  + i*tanh(imag(spic(:,ii))*softscale))/sqrt(2);
                sdfe(:,ii)  = (tanh(real(sdfe(:,ii))*softscale)
                  + i*tanh(imag(sdfe(:,ii))*softscale))/sqrt(2);
```

```
                spic(:,ii)  = Harddecide(spic(:,ii), symlib, Nsym);
                sdfe(:,ii)  = Harddecide(sdfe(:,ii), symlib, Nsym);
            end

            Sym_pic = spic(:,ii);
            Sym_dfe = sdfe(:,ii);


            %% Determining BER for each case of Symbol Estimation
            BER_conv(isiloop,drops,snrloop)
                  = BERcalc(Sym_conv, binarymap, Nsym, QPSK);
            BER_isi(isiloop,drops,snrloop)
                  = BERcalc(Sym_noisi, binarymap, Nsym, QPSK);
            BER_pic(isiloop,drops,snrloop)
                  = BERcalc(Sym_pic, binarymap, Nsym, QPSK);
            BER_dfe(isiloop,drops,snrloop)
                  = BERcalc(Sym_dfe, binarymap, Nsym, QPSK);

        end
    end
    SNR = [SNR snr];
end


%% Extraction of chosen ISI iteration-based BER
ber_conv    = squeeze(sum(BER_conv,2)/Ndrops);
ber_conv    = ber_conv(6,:);
ber_isi     = squeeze(sum(BER_isi,2)/Ndrops);
ber_isi     = ber_isi(6,:);
ber_pic     = squeeze(sum(BER_pic,2)/Ndrops);
ber_pic     = ber_pic(6,:);
ber_dfe     = squeeze(sum(BER_dfe,2)/Ndrops);
ber_dfe     = ber_dfe(6,:);

%% Plotting BER against SNR
plotto(ber_conv, ber_isi, ber_pic, ber_dfe, SNR);
```

SYMBOL GENERATION FUNCTION

```
function [X,sym, binarymap] = SymGen(symlib, QPSK, Nsym, Nfft, CP)

%% Generation of the complete transmitted symbol including the Cyclic
%% Prefix.


sym = zeros(Nfft,1);
randomvalue = ceil(QPSK*rand(Nsym,1));

% Random Allocation of Symbols out of Symbol Library
sym((1+ceil((Nfft-Nsym)/2)):ceil((Nfft+Nsym)/2),:) =
symlib(randomvalue);
Sym = sym/norm(sym);

% Creationg of Symbol Binary Mapping for BER calculation
binarydigits = ceil(log2(QPSK));
binarymap = dec2bin((randomvalue-1),binarydigits);
```

```
% Conversion of Symbol to Time Domain Signal and insertion of CP
X = zeros((Nfft+CP),1);
X((CP+1):length(X),:) = ifft(Sym)*sqrt(Nfft);
X(1:CP,:) = X((Nfft+1):(Nfft+CP),:);
```

HARD DECISION DEVICE FUNCTION

```
function SymOut = Harddecide(Sym, symlib, Nsym)

%% This function implements Hard-Decisions on the processed signals
%% to convert them to actual symbol amplitude levels

Nfft = size(Sym,1);
Sym = Sym((1+ceil(Nfft-Nsym)/2):ceil(Nfft+Nsym)/2,:);

for ii = 1:Nsym
    if (real(Sym(ii,:)) >= 0)
        if (imag(Sym(ii,:)) >= 0)
            symOut(ii,:) = symlib(1);
        else
            symOut(ii,:) = symlib(2);
        end
    else
        if (imag(Sym(ii,:)) >= 0)
            symOut(ii,:) = symlib(3);
        else
            symOut(ii,:) = symlib(4);
        end
    end
end

SymOut = zeros(Nfft,1);
SymOut((1+ceil((Nfft-Nsym)/2)):ceil((Nfft+Nsym)/2),:) = symOut;
```

BER CALCULATION FUNCTION

```
function BER = BERcalc(Sym, binarymap, Nsym, QPSK)

%% This function calculates the BER based on the binary mapping
%% sequence of the actual transmitted symbols

BER = 0;
Nfft = size(Sym,1);

binarydigits = ceil(log2(QPSK));
Sym = Sym((1+ceil(Nfft-Nsym)/2):ceil(Nfft+Nsym)/2,:);

for ii = 1:Nsym
```

```
    if (real(Sym(ii,:)) >= 0)
        if (imag(Sym(ii,:)) >= 0)
            Rxbinary(ii,:) = dec2bin(0,binarydigits);
        else
            Rxbinary(ii,:) = dec2bin(1,binarydigits);
        end
    else
        if (imag(Sym(ii,:)) >= 0)
            Rxbinary(ii,:) = dec2bin(2,binarydigits);
        else
            Rxbinary(ii,:) = dec2bin(3,binarydigits);
        end
    end
end

for ii = 1:Nsym
    BER = BER + sum(sum(abs(binarymap(ii,:) - Rxbinary(ii,:))));
end
```

PLOTTING FUNCTION

```
function plotto(BER1, BER2, BER3, BER4, SNR)

%% This function plots the BER vs. SNR for each of the Symbol
%% estimation cases

QPSK = 4;
Nsym = 128;
binarydigits = ceil(log2(QPSK));


BERry1 = log10((BER1)/(Nsym*binarydigits));
BERry2 = log10((BER2)/(Nsym*binarydigits));
BERry3 = log10((BER3)/(Nsym*binarydigits));
BERry4 = log10((BER4)/(Nsym*binarydigits));

figure(1);
hold on;
plot(SNR, BERry1, '-m', SNR, BERry2, '--r', SNR, BERry3, ':g'
                              , SNR, BERry4, '-.b');
legend('Rcvd. Sig.', 'Post-ISI Removal', 'PIC-Only', 'Post-DFE');
xlabel('SNR (dB)');
ylabel('BER (dB)');
title('Nfft = Ntaps = 128; Nisi = 6; Nici = 4; Scale = 1
                                ; Soft Scale = 2');
```